

2019-02

# Diversity in CO<sub>2</sub> concentrating mechanisms among chemolithoautotrophs from genera *Hydrogenovibrio*, *Thiomicrothrix*, and *Thiomicrospira*, ubiquitous in sulfidic habitats worldwide

Scott, KM

<http://hdl.handle.net/10026.1/12732>

---

10.1128/AEM.02096-18

Applied and Environmental Microbiology

American Society for Microbiology

---

*All content in PEARL is protected by copyright law. Author manuscripts are made available in accordance with publisher policies. Please cite only the published version using the details provided on the item record or document. In the absence of an open licence (e.g. Creative Commons), permissions for further reuse of content should be sought from the publisher or author.*

**Diversity in CO<sub>2</sub> concentrating mechanisms among chemolithoautotrophs from genera *Hydrogenovibrio*, *Thiomicrospira*, and *Thiomicrospira*, ubiquitous in sulfidic habitats worldwide**

Kathleen M. Scott<sup>1#</sup>, Juliana M. Leonard<sup>1</sup>, Rich Boden<sup>2</sup>, Dale Chaput<sup>3</sup>, Clare Dennison<sup>1</sup>, Edward Haller<sup>1</sup>, Tara L. Harmer<sup>4</sup>, Abigail Anderson<sup>1</sup>, Tiffany Arnold<sup>1</sup>, Samantha Budenstein<sup>1</sup>, Rikki Brown<sup>1</sup>, Juan Brand<sup>1</sup>, Jacob Byers<sup>1</sup>, Jeanette Calarco<sup>1</sup>, Timothy Campbell<sup>1</sup>, Erica Carter<sup>1</sup>, Max Chase<sup>1</sup>, Montana Cole<sup>1</sup>, Deandra Dwyer<sup>1</sup>, Jonathon Grasham<sup>1</sup>, Christopher Hanni<sup>1</sup>, Ashlee Hazle<sup>1</sup>, Cody Johnson<sup>1</sup>, Ryan Johnson<sup>1</sup>, Brandi Kirby<sup>1</sup>, Katherine Lewis<sup>1</sup>, Brianna Neumann<sup>1</sup>, Tracy Nguyen<sup>1</sup>, Jonathon Nino Charari<sup>1</sup>, Ooreoluwa Morakinyo<sup>1</sup>, Bengt Olsson<sup>1</sup>, Shanetta Roundtree<sup>1</sup>, Emily Skjerve<sup>1</sup>, Ashley Ubaldini<sup>1</sup>, and Robert Whittaker<sup>1</sup>.

<sup>1</sup>Department of Integrative Biology, University of South Florida, Tampa, Florida, United States of America

<sup>2</sup>School of Biological & Marine Sciences, University of Plymouth, Drake Circus, Plymouth, UK; Sustainable Earth Institute, University of Plymouth, Drake Circus, Plymouth, UK,

<sup>3</sup>Proteomics and Mass Spectrometry Facility, University of South Florida, Tampa, Florida, United States of America,

<sup>4</sup>Biology Program, Stockton University, Galloway, New Jersey, United States of America

#Address correspondences to Kathleen M. Scott, kmscott@usf.edu

Running title: Diverse CCMs in sulfur-oxidizing autotrophs

**ABSTRACT** Members of *Hydrogenovibrio*, *Thiomicrospira* and *Thiomicrothrix* fix carbon at hydrothermal vents, coastal sediments, hypersaline lakes, and other sulfidic habitats. The genome sequences of these ubiquitous and prolific chemolithoautotrophs suggest a surprising diversity of mechanisms for dissolved inorganic carbon (DIC) uptake and fixation; these mechanisms are verified here. Carboxysomes are apparent in transmission electron micrographs of most of these organisms; lack of carboxysomes in *Thiomicrothrix* sp. Milos T2 and *Tmr. arctica*, and an inability to grow under low DIC conditions by *Thiomicrothrix* sp. Milos T2 are consistent with an absence of carboxysome loci in their genomes. For the remaining organisms, genes encoding potential DIC transporters from four evolutionarily distinct families (Tcr0853/0854, Chr, SbtA, SulP) are located downstream of carboxysome loci. Transporter genes collocated with carboxysome loci, as well as some homologs located elsewhere on the chromosomes, had elevated transcript levels under low DIC conditions, as assayed by qRT-PCR. DIC uptake was measureable via silicone oil centrifugation when a representative of each of the four types of transporter was expressed in *Escherichia coli*. Expression of these genes in carbonic anhydrase-deficient *E. coli* EDCM636 enabled it to grow under low DIC conditions, consistent with DIC transport by these proteins. The results from this study expand the range of DIC transporters within the SbtA and SulP transporter families, verify DIC uptake by transporters encoded by Tcr\_0853 and Tcr\_0854 and their homologs, and introduce DIC as a potential substrate for transporters from the Chr family.

**IMPORTANCE** Autotrophic organisms take up and fix DIC, introducing carbon into the biological component of the global carbon cycle. The mechanisms for DIC uptake and

fixation by autotrophic *Bacteria* and *Archaea* are likely to be diverse, but have only been well-characterized among "*Cyanobacteria*". Based on genome sequences, members of *Hydrogenovibrio*, *Thiomicrospira* and *Thiomicrothrix* have a variety of mechanisms for DIC uptake and fixation. We verified that most of these organisms are capable of growing under low DIC conditions, when they upregulate carboxysome loci and transporter genes collocated with these loci on their chromosomes. When these genes, which fall into four evolutionarily independent families of transporters, are expressed in *E. coli*, DIC transport is detected. This expansion in known DIC transporters across four families, from organisms from a variety of environments, provides insight into the ecophysiology of autotrophs, as well as a toolkit for engineering microorganisms for carbon-neutral biochemistries of industrial importance.

**KEYWORDS** CO<sub>2</sub> concentrating mechanism, chemolithoautotroph, autotroph, carbon fixation

## (INTRODUCTION)

Autotrophic members of domains *Bacteria* and *Archaea* are responsible for introducing carbon into the biological portion of the global carbon cycle in virtually any habitat with sufficient light or chemical energy to power the process of carbon fixation. They use CO<sub>2</sub> from the air, or dissolved inorganic carbon (DIC = CO<sub>2</sub> + HCO<sub>3</sub><sup>-</sup> + CO<sub>3</sub><sup>2-</sup>), if aquatic, as their carbon source, and have a variety of mechanisms to compensate for variability in the availabilities of these compounds.

CO<sub>2</sub>-concentrating mechanisms (CCMs) are one such mechanism, and have been particularly well-studied among members of the phylum "*Cyanobacteria*". In these organisms, active transport of HCO<sub>3</sub><sup>-</sup> elevates its intracellular concentration.

Cytoplasmic HCO<sub>3</sub><sup>-</sup> enters carboxysomes. These protein-bound microcompartments contain the enzymes carbonic anhydrase (EC 4.2.1.1), and ribulose 1,5-bisphosphate carboxylase/oxygenase (RubisCO, EC 4.1.1.39). These enzymes act together to dehydrate some of the HCO<sub>3</sub><sup>-</sup> to form CO<sub>2</sub>, and use the CO<sub>2</sub> to carboxylate ribulose bisphosphate, leading to the formation of 3-phosphoglycerate for biosynthesis (1-3).

The HCO<sub>3</sub><sup>-</sup> transporters characterized in members of phylum "*Cyanobacteria*" fall into three evolutionarily independent lineages: BCT1, an ABC transporter (4); BicA, a member of the SulP family of transporters (5); and SbtA (6). Loss of cytoplasmic DIC is minimized by conversion of cytoplasmic CO<sub>2</sub> to HCO<sub>3</sub><sup>-</sup> via membrane-associated carbonic anhydrases, which couple CO<sub>2</sub> hydration to redox reactions (7, 8). This arsenal of DIC transporters and traps is distributed among members of "*Cyanobacteria*" based on their habitats; those inhabiting freshwater and sediments, in which DIC concentration and composition can vary most greatly (e.g., due to pH differences) tend

to carry a variety of these complexes, while those inhabiting the open ocean, where DIC concentrations and pH values are subject to much less variation, tend to carry a more limited subset (9). For organisms carrying a variety of transporters and traps, these complexes are differentially regulated in a manner consistent with differences in their parameters (e.g., higher-affinity transporters BCT1 and SbtA are favored when  $\text{HCO}_3^-$  concentrations are particularly low (1)).

CCMs are not well-characterized among autotrophs from the many other phyla of *Bacteria* and *Archaea* with autotrophic members. Carboxysomes are present in many autotrophic members of *Alpha*-, *Beta*-, and *Gammaproteobacteria*, and their structure and function have been well-characterized for *Halothiobacillus neapolitanus* Parker  $X^T$  from the *Chromatiales* of the *Gammaproteobacteria* (10-12). DIC uptake has only been studied in detail for *Hydrogenovibrio crunogenus*, a sulfur-oxidizing chemolithoautotroph from the *Thiotrichales* of the *Gammaproteobacteria*, isolated from deep-sea hydrothermal vents (13). This organism generates elevated intracellular DIC concentrations in an energy-dependent manner (14, 15), and has carboxysomes (16), which likely facilitates its ability to grow rapidly under low-DIC conditions (14). Random and site-directed mutagenesis of gene loci Tcr\_0853 and Tcr\_0854, which are located downstream of the carboxysome locus in this organism, result in a high- $\text{CO}_2$  requiring phenotype, and loss of an ability to generate high intracellular concentrations of DIC, suggesting that these genes encode a two-component DIC transporter (17). Homologs of these genes are common among autotrophic *Bacteria*, and one of them (Tcr\_0854) is from a PFAM without prior biochemical characterization (PFAM10070; (17)).

Several members of *Thiomicrospira*, *Thiomicrothrix*, and *Hydrogenovibrio*, organisms taxonomically affiliated with *H. crunogenus* (18), have had their genomes sequenced. Taxa were selected for sequencing to represent both the taxonomic breadth of these genera, as well as the range of habitats from which these organisms have been isolated, including shallow and deep-sea hydrothermal vents, coastal sediments, and soda and salt lakes (19). Despite the rather narrow taxonomic range of the organisms sequenced, a surprising diversity in mechanisms for DIC uptake and fixation was suggested from the genome data. Genome sequences of some members of *Thiomicrothrix* lack carboxysome loci altogether, suggesting the absence of a CCM. For members of *Thiomicrospira*, genes encoding carboxysome components are present, but those encoding carboxysomal carbonic anhydrase are lacking. Instead, they each carry a gene in its place without apparent homologs beyond this genus (19), raising the possibility that these genes might encode a novel form of carboxysomal carbonic anhydrase. In all cases, when present, carboxysome loci are followed by genes encoding transporters from four evolutionarily distinct families. Carboxysome locus-associated genes encoding potential transporters include homologs to those encoding the potential DIC transporter in *H. crunogenus* (Tcr\_0853, Tcr\_0854), and members of the SulP and SbtA families distantly related to those known to transport  $\text{HCO}_3^-$  in members of "*Cyanobacteria*". Also included are members of the Chr family, which is widely distributed among prokaryotes. The two biochemically characterized members of this family confer resistance to chromate by extruding this anion, perhaps functioning as a chromate/sulfate antiporter (20).

The unexpected diversity in mechanisms for DIC uptake and fixation suggested by genome data from members of *Thiomicrospira*, *Thiomicrothrix*, and *Hydrogenovibrio*, was verified here. Carboxysome presence or absence was confirmed via transmission electron microscopy. To determine whether the genes encoding potential DIC transporters might facilitate growth under low-DIC conditions, their transcription patterns were monitored, and representative members of all four potential DIC transporter families were heterologously expressed in *E. coli* to verify an ability to transport DIC.

## RESULTS

**Genome context of carboxysome loci, and phylogenetic analysis of genes encoding potential DIC transporters.** Carboxysome loci are present in the genomes of most of the organisms studied here (available at Integrated Microbial Genomes and Microbiomes <https://img.jgi.doe.gov/>). The genome sequences of *Tmr. arctica* and *Thiomicrothrix* sp. Milos-T2 lack carboxysome loci (19); either these loci are absent, or they are present in a portion of the genome which has yet to be sequenced. Genomes from all four sequenced members of *Thiomicrothrix* were scrutinized for evidence of genome rearrangement in the region associated with the carboxysome locus. For *Tmr. frisia* KP2 and *Tmr. chilensis*, genome synteny was conserved upstream and downstream of the carboxysome locus (Fig. 1). These conserved regions were also present in *Tmr. arctica* and *Thiomicrothrix* sp. Milos-T2, but without the intervening carboxysome locus. These data are consistent with carboxysome locus loss in these two taxa.



For the other organisms, phylogenetic analyses were conducted on genes encoding potential DIC transporters from the regions immediately downstream from the carboxysome loci, along with homologs to these genes present elsewhere in these genomes and others (Fig. 2; Fig. 3; Figs. S1-S5 depict sequence logos derived from alignments of these genes). For all four types of potential transporters, genes from the organisms studied here fell into multiple, distinct and distant clades: 2 clades for homologs to Tcr\_0853 and 0854, 3 clades for Chr, 2 clades for SbtA, and 4 clades for SulP. Homologs of SulP, SbtA, and the two-component transporter from *H. crunogenus* are often collocated with carboxylases and other enzymes that consume DIC (Fig. 2; Fig. 3) which suggests a role in DIC uptake for them.

**Growth under low-DIC conditions, and DIC concentrations *in situ*.** All taxa tested here grew under high-DIC conditions; all but *Thiomicrothrix* sp. Milos-T2 were capable of growth under low-DIC conditions (2 mM DIC under ~400 ppm CO<sub>2</sub> ambient headspace; Fig. 4). *Tmr. arctica* lacks genes encoding carboxysomes; therefore, growth under low-DIC conditions was unexpected, motivating further consideration of its habitat. CO<sub>2</sub> concentrations estimated for the marine Arctic sediments from which *Tmr. arctica* was isolated are lower than those at the hydrothermal vent habitat from which *H. crunogenus* was isolated (Table 1).

**Carboxysome presence and differential expression.** When cells were incubated under low-DIC conditions, carboxysomes were apparent in transmission electron micrographs of all taxa whose genomes encode these microcompartments, and were absent in *Tmr. arctica* and *Thiomicrothrix* sp. Milos-T2 (Fig. 5).

Transcripts from genes present in carboxysome loci were more abundant when cells were cultivated under low-DIC conditions (Table 2), which is consistent with the role of carboxysomes in CCMs to facilitate growth under low-DIC conditions (21). Carboxysome-associated genes did not have as large a change in transcript abundance in *Tms. pelophila*, and transcripts from the gene N746DRAFT\_0321 (*hyp(csoS2)*, Table 2), were undetectable under low-DIC conditions.

#### **Response of transporter transcript abundances to DIC concentration.**

Transcript levels from many genes encoding potential DIC transporters were significantly different when cells were grown under low-DIC versus high-DIC conditions (Table 2; two-tailed *t*-test,  $\alpha < 0.05$ ,  $-\Delta\Delta C_t = 0$ ). Many of these genes were upregulated under low-DIC conditions, with  $-\Delta\Delta C_t > 1$ , indicating that transcript levels were at least doubled under low-DIC conditions (Table 2; one-tailed *t*-test,  $\alpha < 0.05$ ).

Under low-DIC conditions, all genes assayed here encoding members of two distinct clusters within the SbtA family, and two clusters of homologs of the Tcr\_0853/0854-encoded transporter from *H. crunogenus* (17), were upregulated, whether adjacent to carboxysome loci or not (Table 2). When genes encoding members of the Chr and SulP families were adjacent to carboxysome loci, they were also upregulated under low-DIC conditions (Table 2). When located elsewhere on the chromosome, some members of the SulP family were upregulated, but members of Chr not associated with carboxysomal loci were not.

#### **DIC uptake activity of heterologously expressed transporters.** Genes

encoding members of all four families of potential DIC transporters were selected for

heterologous expression based on collocation with the carboxysome locus and upregulation under low-DIC conditions (Table 2): the two-component transporter from *H. crunogenus* XCL-2 (Tcr\_0853, Tcr\_0854), members of Chr and SulP transporter families from *H. thermophilus* JR2, and a member of the SbtA transporter family from *Tmr. frisia* KP2. Mass spectrometric analysis of proteins from membranes from *E. coli* constructs expressing these transporters verified their expression (Table 3). Signal intensity was always low for the protein product of Tcr\_0853, which may reflect that this protein is likely to be particularly hydrophobic (11 predicted membrane-spanning alpha helices), and therefore more difficult to solubilize, digest, elute from the C<sub>18</sub> column used to resolve the peptides, and ionize for mass spectrometry.

*E. coli* expressing these genes were able to generate elevated intracellular DIC concentrations (Fig. 6; Fig. S6). Intracellular DIC was similar to extracellular when putative DIC transporters were oriented in reverse relative to the T7 promotor driving their expression. When genes were correctly oriented relative to the T7 promoter, intracellular DIC concentrations were higher than when in reverse orientation (Fig. 6; for *sbtA*, *chr*, *sulP*: two-tailed *t*-test, F versus R orientations,  $\alpha < 0.05$ ; for 8534 (F), 8534(R), 853(F), 854(F): ANOVA, with post-hoc multiple comparisons via Scheffe, Bonferroni, and Tukey tests;  $\alpha < 0.05$  for 8534 (F)). Intracellular DIC was particularly high for cells expressing SbtA. The presence of both Tcr\_0853 and Tcr\_0854 were necessary for the accumulation of intracellular DIC, suggesting that the gene products of both are required for DIC uptake, and that they may form a two-subunit transporter. The presence of *chr* in the forward orientation relative to the promotor did result in

elevated DIC concentrations compared to when it was in the reverse orientation, but intracellular concentrations were lower than for the other transporters (Fig. 6, Fig. S6).

Expression of all four types of transporter genes in *E. coli* EDCM636 enabled this carbonic anhydrase-deficient strain (22) to grow under an atmosphere of ~400 ppm CO<sub>2</sub> (Fig. 7). Cells expressing both Tcr\_0853 and Tcr\_0854 grew more rapidly than those expressing either of these genes individually, in reverse orientation, or in the absence of IPTG (Fig. 7A). Cells expressing *chr* only grew when this gene was in the forward orientation relative to the T7 promotor. This growth was preceded by a very long lag period, perhaps due to the very low levels of DIC transport measured in cells expressing this gene (Fig. 6). In replicate experiments, it was not clear whether the presence of IPTG stimulated growth (Fig. 7B, 7C). Cells expressing *sbt* and *sulP* grew most rapidly when in the forward orientation relative to the T7 promotor and when IPTG was added to the growth medium (Fig. 7D, E). Growth in the absence of IPTG may have been due to background expression of T7 RNA polymerase (23).

## DISCUSSION

Strategies for coping with growth under low-DIC conditions are quite diverse among members of *Thiomicrospira*, *Thiomicrothrix*, and *Hydrogenovibrio*. While most strains queried here appear to have CCMs, two do not. For those taxa that do have CCMs, there are variations in carboxysome loci and transporter genes associated with these loci that suggests a surprising heterogeneity among the CCMs of these organisms.

*Tmr. arctica* and *Thiomicrorhabdus* sp. Milos-T2 do not appear to have CCMs, based on an absence of carboxysome loci and homologs to most of the transporter genes associated with these loci. The inability of *Thiomicrorhabdus* sp. Milos-T2 to grow under low-DIC conditions is consistent with these genome traits. In contrast, growth by *Tmr. arctica* under low-DIC conditions was surprising. This organism may have a novel mechanism for growing under low-DIC conditions. Alternatively, its growth may be facilitated by higher CO<sub>2</sub> concentrations that result from the lower temperatures at which this organism grows, since lower temperatures increase the solubility of CO<sub>2</sub>, and also increase the pK<sub>a</sub> of bicarbonate (24). However, these physical and chemical factors do not appear likely to result in particularly high concentrations of CO<sub>2</sub> in the habitat from which *Tmr. arctica* was isolated (Table 1). Perhaps the lower maximum specific growth rates observed for this psychrophilic organism (25), may render carboxysomes and CCMs unnecessary.

The branching order predicted from supertrees constructed for members of *Thiomicrospira*, *Thiomicrorhabdus*, and *Hydrogenovibrio* (18, 19); Fig. 1) suggests that the loss of carboxysome loci may have occurred independently in the lineages leading to *Tmr. arctica* and *Thiomicrorhabdus* sp. Milos-T2. CCMs may not have provided a selective advantage for these organisms. Given the size of carboxysomes, as well as their abundance when expressed (21), carboxysome loss would provide an energetic advantage for cells growing in habitats with consistently elevated concentrations of CO<sub>2</sub>. *Thiomicrorhabdus* sp. Milos-T2 was cultured from the same hydrothermal vent system as *Hydrogenovibrio* sp. Milos-T1 (26), which has a carboxysome locus. Perhaps they inhabit different niches with different CO<sub>2</sub> abundances in this system.

Carboxysome loci in members of *Thiomicrospira* are unusual in their lack of genes encoding carboxysomal carbonic anhydrase (*csoSCA*), distinguishing them from those present in members of *Thiomicrothrix* and *Hydrogenovibrio*, as well as many other members of the "*Protoeobacteria*" (27). Orthologs to genes encoding carboxysomal carbonic anhydrase are entirely absent from their genomes. In *Tms. pelophila*, the locus N746DRAFT\_0321 (IMG gene object ID 2568509999), located at the position in the carboxysomal locus usually occupied by *csoSCA*, does not appear to be transcribed under low-DIC conditions (Table 2, *hyp(csoS2)*). Based on this transcription pattern, it is unlikely that this locus encodes a protein that could fulfil the role of carboxysomal carbonic anhydrase under low-DIC conditions. It is possible that the carboxysomes in these organisms function without carbonic anhydrase activity.

Heterologously expressed members of all four transporter families associated with carboxysome loci are capable of DIC uptake (Fig. 6, Fig. 7). These measurements verify DIC uptake by the proteins encoded by Tcr\_0853 and Tcr\_0854. They expand DIC uptake by SbtA-family transporters to the product of the *sbtA* gene from *Tmr. frisia* KP2, whose predicted amino acid sequence is only 28 to 29% identical to biochemically characterized SbtA-family bicarbonate transporters from "*Cyanobacteria*". Likewise, it also broadens the known distribution of DIC transporters within the SulP-family transporters; the SulP protein from *Hydrogenovibrio thermophilus* JR2 is only 23% identical to the SulP-family bicarbonate transporter from *E. coli*, and only 19 - 21% identical to SulP-family bicarbonate transporters from "*Cyanobacteria*". It also adds DIC transport as a potential function for members of Chr. Perhaps these transporters have differences in affinities for DIC, transport different forms of DIC ( $\text{CO}_2$ ,  $\text{HCO}_3^-$ ,  $\text{CO}_3^{2-}$ ), or

have different mechanisms for transport (e.g., symport with cations; antiport with anions), which provide advantages for their activities under specific growth conditions.

DIC uptake by some transporters from "*Cyanobacteria*" cannot be successfully assayed by silicone oil centrifugation and complementation of growth of carbonic anhydrase-deficient *E. coli* (28). Perhaps shared membership with *E. coli* in the class *Gammaproteobacteria*, or the stronger T7 promoter used for expression here, were responsible for successful heterologous expression and activity. Successful heterologous expression of the genes studied here bodes well for their potential use in constructing organisms capable of synthesizing industrially relevant precursor compounds from CO<sub>2</sub> and HCO<sub>3</sub><sup>-</sup>.

Multiple clades of each transporter family are present among the organisms studied here. Among these organisms, homologs to Tcr\_0853 and 0854, as well as SbtA, fall into two clades each. In both cases, most of the genes fall together into a single well-supported clade. Genes outside of this clade fall among those present in distantly related members of "*Proteobacteria*", and organisms carrying these genes also carry a copy falling within the clade. These 'extra copies' could have been relatively recently acquired via horizontal gene transfer. Representatives from both clades from both transporter families all have elevated transcript levels when cells are grown under low-DIC conditions. Furthermore, genes encoding these two types of transporters are usually present adjacent to genes encoding CO<sub>2</sub>-metabolizing enzymes (Fig. 2; Fig. 3); this colocation, as well as upregulation under low CO<sub>2</sub> conditions suggests that members of these transporter families may predominantly transport DIC.

The only members of the Chr and SulP families to have elevated transcript levels under low-DIC conditions fell within a single clade of each family (Table 2; Fig. 2; Fig. 3). The members of the Chr and SulP families tested here whose transcript levels were not sensitive to DIC concentrations and are not collocated with carboxysome genes may not play a role in CCMs, and may instead be either constitutively expressed DIC transporters, or transport sulfate or other cations. Few members of these transporter families are collocated with genes encoding CO<sub>2</sub>-metabolizing enzymes (Fig. 2; Fig. 3), suggesting that roles in DIC uptake may be less widespread in these transporter families. However, it is important to note that a SulP-family transporter has been implicated in DIC uptake in *E. coli* (5, 29).

The SulP-family transporters studied here have domains that distinguish them from other members of this transporter family. Similar to the SulP transporters present in "*Cyanobacteria*", they lack the  $\beta$ -carbonic anhydrase domain found in some members of this family. When present in other organisms, this carbonic anhydrase domain is located on the cytoplasmic side of the cell membrane. This absence of a carbonic anhydrase domain is consistent with transporting HCO<sub>3</sub><sup>-</sup> into the cytoplasm to generate elevated DIC concentrations there; if it were present, a carbonic anhydrase domain would convert the transported HCO<sub>3</sub><sup>-</sup> into CO<sub>2</sub> at the cell membrane, where it would diffuse out of the cell (30). Unlike those present in "*Cyanobacteria*", the SulP-family transporters found in the organisms studied here lack the carboxy-terminal STAS domain typically found in SulP proteins. The STAS domain is hypothesized to regulate the activities of these transporters (31, 32). HCO<sub>3</sub><sup>-</sup> transporters in "*Cyanobacteria*" are post-translationally regulated, and inactive in the dark (reviewed in (33)). Though this



particular mechanism, STAS-domain mediated post-translational regulation, is absent for the SulP proteins studied here, it is still possible that the CCMs of these organisms could be post-translationally regulated, which would provide them with an advantage given the temporal heterogeneity of the habitats from which they were isolated (e.g., hydrothermal vents (34)).

The presence of multiple DIC transporter genes in many of the organisms studied here, and their variability in collocation with the carboxysome locus, provide a basis for a model of DIC transporter gene acquisition, loss, and changes in chromosome location. Based on its chromosomal location in members of *Thiomicrospira*, *Thiomicrothrix*, and *Hydrogenovibrio*, it seems likely that an SbtA-family transporter was collocated with the carboxysome locus in the shared ancestor of these three genera (Fig. 8). In this scenario, members of the other three transporter families were encoded elsewhere in the genomes of all three genera, and displaced members of SbtA in many taxa (e.g., orthologs to Tcr\_0853 and 0854 (853&4-I); *chr-I*; Fig. 8). Acquisition of a second copy of homologs to Tcr\_0853 and 0854 by the lineage leading to *Hydrogenovibrio* sp. Milos-T1 was likely via horizontal gene transfer, given its placement among genes from more distantly related organisms (Fig. 2A). The selective advantage of placing DIC transporter genes adjacent to those encoding carboxysome genes is not apparent, as transporter genes positioned elsewhere on the chromosome are also upregulated under low DIC conditions (e.g., Tcr\_0853 and 0854 homologs in *H. thermophilus* JR-2 and MA2-6, *Hydrogenovibrio* sp. Milos-T1, and *Tms. pelophila*; Table 2). Functional characterization of these different types of transporters, as well as a

more detailed examination of the growth conditions under which they are upregulated, may clarify the forces driving selective pressure for their positions on the chromosome.

## MATERIALS AND METHODS

**Phylogenetic analysis of genes encoding potential DIC transporters.** Transporter genes and their homologs were collected from the Integrated Microbial Genomes and Microbiomes (IMG/M) database (35). Amino acid sequences predicted from the genes were aligned via MUSCLE (36), and sequence logos were generated from the alignments via Weblogo (<http://weblogo.berkeley.edu/>) (37). Alignments were refined via GBLOCKS with stringent criteria (38). Phylogenetic trees were constructed in PhyML 3.0 (39) using Maximum Likelihood (ML) analysis. Smart Model Selection (SMS) in PhyML 3.0 (40) was used to evaluate best-fit models of evolution (853/854: LG +G+I+F, G = 0.888, I = 0.144; Chr: LG +G +F, G = 0.869; SbtA: LG + G + I + F, G = 1.043; I = 0.072; SulP: LG +G +F, G = 1.365; LG = Le and Gascuel model; G = gamma distribution parameter; I = proportion of invariant sites; F = amino acid frequencies estimated from the sequences (41)). Results were assessed using 1000 bootstrap replicates, and the consensus tree was visualized using FigTree (Version 1.4.3; (42)).

**Growth under low and high-DIC conditions.** Organisms were obtained from the Deutsche Sammlung von Mikroorganismen und Zellkulturen (DSMZ):

*Hydrogenovibrio crunogenus* XCL-2 DSM 25203, *Hydrogenovibrio thermophilus* JR2 DSM 25194, *Hydrogenovibrio thermophilus* MA2-6 DSM 13155, *Hydrogenovibrio halophilus* DSM 15072<sup>T</sup>, *Hydrogenovibrio kuenenii* DSM 12350, *Hydrogenovibrio marinus* DSM 11271<sup>T</sup>, *Hydrogenovibrio* sp. Milos-T1 DSM 13190, *Thiomicrothrix*

380 *frisia* Kp2 DSM 25197, *Thiomicrorhabdus* sp. Milos-T2 DSM 13229, *Thiomicrorhabdus*  
 381 *chilensis* DSM 12352, *Thiomicrorhabdus arctica* DSM 13458, *Thiomicrospira pelophila*  
 382 DSM 1534<sup>T</sup>.

383 To test for ability to grow under low-DIC conditions, organisms were cultivated at  
 384 20°C in thiosulfate-supplemented artificial seawater (TASW; (14), pH 7.5, 15 µg/L  
 385 vitamin B-12). For *H. halophilus*, NaCl was raised to 1.5 M (43), and for *Tmr. arctica*, the  
 386 culture temperature was 10°C. High DIC cultures (50 mM NaHCO<sub>3</sub>, 5% headspace  
 387 CO<sub>2</sub>) in TASW were used to inoculate paired flasks containing high DIC and low-DIC  
 388 medium (2 mM NaHCO<sub>3</sub>, 0.04% ambient air headspace CO<sub>2</sub>; one low-DIC and high-DIC  
 389 culture per strain). Turbidity was monitored at 600 nm.

390 **Estimation of DIC concentrations present in microorganism habitats.** To  
 391 estimate DIC concentrations in Arctic sediments for comparison with those present at  
 392 hydrothermal vents, DIC speciation was modelled in PHREEQC Interactive 3.3.12 (US  
 393 Geological Survey, (44)) using the Lawrence Livermore National Laboratory database  
 394 (llnl.dat, based in part on the EQ3/6 model (45)). Seawater inorganic ion composition  
 395 was based on that of (46). For the Arctic samples, the initial pH was 8.22 (2.32 mM  
 396 DIC), and the model was run on the basis of water without air equilibration or a gas-  
 397 phase present, at 0.01 or 6°C, and 17.7 atm (168 m depth). For vent samples, the initial  
 398 pH was either 7.20 (2.7 mM DIC) or 5.6 (7.1 mM DIC) and 206.8 atm (2,075 m depth).

399 **Transmission electron microscopy of carboxysomes.** Cells were cultivated  
 400 to verify carboxysome presence in these taxa. Since *Thiomicrorhabdus* sp. Milos-T2  
 401 did not grow under low-DIC conditions (see results), a two-stage process was used to

induce carboxysome synthesis in all organisms tested (16). First, cells were cultivated under high-DIC conditions (see above). Cells were harvested from these cultures via centrifugation, and resuspended in low-DIC TASW medium. After incubating in low-DIC medium overnight, cells were centrifuged, preserved with 2.5% glutaraldehyde, and prepared for transmission electron microscopy as in (16).

**qRT-PCR assay of transcript abundances from genes encoding carboxysome components and potential DIC transporters.** To determine whether carboxysome-associated transporter gene transcripts were more abundant when cells were grown under low-DIC conditions, taxa that were amenable to cultivation in chemostats were grown under two conditions: DIC limitation (low-DIC), and NH<sub>3</sub> limitation (high-DIC; (14). Cells were harvested via centrifugation (10,000 × *g*, 5 min, 4°C), flash-frozen with liquid nitrogen, and stored at -80°C for subsequent RNA extraction using the Ambion RiboPure-Bacteria Kit (17). Primers were designed to target genes encoding carboxysome components (*csoS2*; *csoS3*; positive control for CCM induction), citrate synthase (calibrator for the  $2^{-\Delta\Delta C_t}$  method; (47), and transporters (Table 4), and qRT-PCR assays were implemented in an Applied Biosystems Step One real-time PCR system, using QuantiTect SYBR Green RT-PCR (Qiagen, Inc.) as described in (17).

**Heterologous expression of potential DIC transporters.** Genes representing all four families of potential DIC transporters were selected from *H. crunogenus* XCL-2 (Tcr\_0853, Tcr\_0854), *H. thermophilus* JR2 (Chr and SulP), and *Tmr. frisia* KP2 (SbtA). Genomic DNA was purified as in (19), and PCR primers were designed to amplify genes and heterologously express them with native amino and carboxy termini (Table

5). High-fidelity Platinum SuperFi DNA polymerase (Invitrogen; Carlsbad, CA) was used as recommended by manufacturer. PCR products were cloned into pET101/D-TOPO vector, and transformed into OneShot TOP10 competent cells (Invitrogen; Carlsbad, CA). Plasmids were purified from transformed cells, and the sequence and orientation of the target genes was verified (Macrogen USA; Rockville, MD). Most constructs were oriented in the forward direction relative to the vector T7 promoter. For constructs with SbtA and both Tcr\_0853 and Tcr\_0854, some clones had these genes in reverse orientation relative to the T7 promoter. These were used as negative controls. Constructs with *chr* and *sulP* genes in reverse orientation were generated using PCR primers that would orient them as such relative to the promoter (Table 5). Plasmids were transformed into *E. coli* strain Lemo21(DE3) (New England Biolabs, Ipswich, MA), which has been optimized for membrane transporter expression by modulating T7 RNA polymerase activity with a rhamnose-inducible inhibitor for this enzyme (48, 49). Expression, as assayed by DIC uptake (see description of silicone oil centrifugation below), was optimized by growing each strain in the presence of a range of rhamnose concentrations (0 – 2 mM), inducing gene expression with 0.4 mM isopropyl  $\beta$ -D-1-thiogalactopyranoside (IPTG), and harvesting at a range of times (4-24 hours post-induction).

*E. coli* carrying genes encoding potential DIC transporters were cultivated on a gyrotary shaker (150 rpm, 37°C) in lysogeny broth supplemented with 100 mg/L ampicillin and 30 mg/L chloramphenicol. Since rhamnose addition was not found in pilot experiments to enhance expression of the target genes, it was not added to the growth media. When OD<sub>600</sub> reached 0.5 – 1.2, IPTG was added (0.4 mM), and cells

were cultivated for another four hours at 30°C. Cells were harvested (10,000 × g 5 min, 4°C). For proteomic analysis, cells were stored at -20°C. For DIC uptake assays, cells were resuspended in fresh medium (OD<sub>600</sub> ~50 0.4 mM IPTG) and stored on ice until use, within 1 hr of harvest.

**Membrane preparations and proteomics.** To verify heterologous expression of the potential DIC transporter genes, membranes were prepared from *E. coli* grown as described above. Pellets from 20 ml cultures were thawed and resuspended in 10 ml membrane buffer (50 mM TRIS pH 8, 10 mM EDTA) supplemented with chicken egg lysozyme (0.1 mg/ml), and incubated for 30 min at 20°C. Lysate was sonicated on ice for 15 sec to decrease viscosity, and centrifuged to remove debris and intact cells (6,000 × g, 30 min, 4°C). Supernatant was centrifuged to pellet the membranes (75,000 × g, 30 min, 4°C). Pellets (membranes) were rinsed twice with membrane buffer.

Membrane pellets were then resuspended in SDS-PAGE sample buffer. Instead of heating to 95°C, which can cause membrane proteins to aggregate (50), samples were incubated at 37°C for 1 hr to facilitate dissolution before subjecting them to SDS-PAGE (51). Coomassie-stained gel fragments were excised from the molecular weight region corresponding to those predicted from the amino acid sequence of the target protein, and processed as described previously (17).

Peptides were separated using a 50cm C<sub>18</sub> reversed-phase-HPLC column on an Ultimate3000 UHPLC system (Thermo Fisher Scientific) with a 60 minute gradient (4-40% acetonitrile with 0.1% formic acid) and analyzed on a hybrid quadrupole-Orbitrap instrument (Q Exactive Plus, Thermo Fisher Scientific) using data-dependent acquisition, where the top 10 most abundant ions were selected for MS/MS analysis in

the linear ion trap. Raw data files were processed in MaxQuant (version 1.6.1.0, [www.maxquant.org](http://www.maxquant.org)) and searched against the *H. crunogenus* Uniprot proteome, which had been modified to also include the amino acid sequences predicted from the *H. thermophilus* JR2 and *Tmr. frisia* KP2 genes that were cloned, using search parameters and filtering criteria as in (17).

**DIC uptake activity of heterologously expressed transporters.** As in (28), two approaches were taken to determine whether the heterologously expressed transporters were capable of DIC uptake: silicone oil centrifugation and complementation of growth of carbonic anhydrase-deficient *E. coli*. Silicone oil centrifugation was used to assay DIC uptake as described (14). 10  $\mu$ l portions of suspended cells were added to 200  $\mu$ l lysogeny broth, 50 mM HEPES pH 8, 0.25 mM  $\text{DI}^{14}\text{C}$  (2 mCi/ml  $\text{NaH}^{14}\text{CO}_3$ , 15 mCi/mmol; MP Biomedicals, Inc., Irvine, CA). These 200  $\mu$ l suspensions were layered on top of microcentrifuge tubes preloaded with a dense killing solution overlain by silicone oil (14). Timecourses were run to determine how long to incubate the cells before centrifugation into the killing solution to assay  $\text{DI}^{14}\text{C}$  uptake. Based on these pilot experiments, incubations of 90 sec were used. At 90 sec, microcentrifuge tubes were centrifuged at maximum speed (14,000  $\times g$ ) for 30 sec before processing as described in (14). Cell-free controls were run in parallel with the samples, and  $^{14}\text{C}$  counts from these controls ( $^{14}\text{C}$  accumulation in the killing solution due to e.g.,  $^{14}\text{CO}_2$  diffusion) were subtracted from counts measured when cells were present. Cell volumes (cytoplasm plus periplasm) were determined via silicone oil centrifugation by incubating cells in the presence of tritiated water (3  $\mu\text{Ci}/\text{ml}$ , Amersham Biosciences, Little Chalfont, UK). Cytoplasm volumes were calculated from cell

volumes by assuming they were 92% of cell volume (52). 2-tailed t-tests were used to determine whether DIC concentrations differed in cells expressing genes in forward versus reverse orientation relative to the T7 promoter. For cells expressing Tcr\_0853, Tcr\_0854, or both, differences in intracellular DIC concentrations were tested for significance with ANOVA, using Scheffe, Bonferroni, and Tukey tests for post-hoc multiple comparisons. Statistical tests were implemented in IBM SPSS Statistics version 24.

*E. coli* EDCM636 is only capable of growth under high DIC conditions due to disruption of its  $\beta$ -carbonic anhydrase gene with a kanamycin resistance cartridge (22). When genes encoding DIC transporters from "*Cyanobacteria*" are expressed by this strain, it is capable of growing under ambient atmosphere (~400 ppm CO<sub>2</sub>; (28). A culture of this strain was obtained from the Coli Genetic Stock Center at Yale University to screen transporters for DIC uptake activity. Unlike (28), in which DIC transporter expression was driven by the *lac* promoter, target gene expression in this study was driven by the T7 promoter. Since the transporter genes carried on pET101/D-TOPO (described above) require T7 RNA polymerase for expression, it was necessary to introduce a derivative of plasmid pAR1219 carrying an IPTG-inducible copy of the gene encoding this enzyme (53) into *E. coli* EDCM636. Since both pET101/D-TOPO and pAR1219 confer resistance to ampicillin, it was necessary to modify pAR1219 beforehand by interrupting its beta lactamase gene with a trimethoprim resistance cartridge using the EZ-Tn5 <DHFR-1> insertion kit (Epicentre). Chemically competent *E. coli* EDCM636 were transformed first with modified pAR1219 (conferring trimethoprim resistance, but not ampicillin resistance). These cells were subsequently



transformed with pET101/D-TOPO plasmids carrying candidate DIC transporters, and screened for an ability to grow under low DIC conditions. Lysogeny broth (100 mg/L ampicillin, 50 mg/L kanamycin, 50 mg/L trimethoprim) was inoculated with each strain, and 5-fold serial dilutions were prepared for each. These overnight cultures were grown overnight under a headspace of 5% CO<sub>2</sub>. Since pseudo-revertants capable of growing under low-DIC conditions are frequent in *E. coli* EDCM636 (22, 28), the highest-titer overnight culture was divided into two equal portions. One portion was incubated under 5% CO<sub>2</sub> with the other cultures, while the other was incubated under ambient air overnight. The next morning, the absence of growth for the culture incubated under ambient air was verified. The optical density of the serial dilutions incubated under 5% CO<sub>2</sub> was measured, and cultures with OD<sub>600</sub> = 0.3 – 0.5 were selected to be used as inocula. These cultures were split into two portions, one was brought to 0.4 mM IPTG, and all were incubated another hour under 5% CO<sub>2</sub>. Each was then added 1:100 v/v to three portions of fresh lysogeny broth supplemented with the antibiotics described above, plus 0.4 mM IPTG as appropriate for the experiment. These cultures were incubated (30°C, 150 rpm) under ambient atmosphere and monitored for growth spectrophotometrically at 600 nm.

## SUPPLEMENTAL MATERIAL

**FIG S1** Sequence logo from the alignment of Tcr\_0853 homologs used to construct the phylogenetic tree in Fig. 2A.

**FIG S2** Sequence logo from the alignment of Tcr\_0854 homologs used to construct the phylogenetic tree in Fig. 2A.

**FIG S3** Sequence logo from the alignment of Chr family transporters used to construct the phylogenetic tree in Fig. 2B.

**FIG S4** Sequence logo from the alignment of SbtA family transporters used to construct the phylogenetic tree in Fig. 3A.

**FIG S5** Sequence logo from the alignment of SulP family transporters used to construct the phylogenetic tree in Fig. 3B.

**FIG S6** Intracellular DIC accumulation by *E coli* expressing potential DIC transporter genes A) Tcr\_0853, Tcr\_0854, *sulP*, or *chr*, and B) *sbtA* from pilot experiments.

## ACKNOWLEDGMENTS

We are grateful for support from the National Science Foundation ((NSF-IOS-1257532 to K.M.S.) and the University of South Florida Pilot Studies Awards program. We are also grateful to Gordon Cannon for discussion and comments on an earlier version of this manuscript, as well as the insightful comments of the anonymous reviewers of this manuscript. Author contribution statement: KMS designed the study; all authors conducted experiments, and contributed to data analysis and writing the manuscript.

## REFERENCES

1. **Price GD.** 2011. Inorganic carbon transporters of the cyanobacterial CO<sub>2</sub> concentrating mechanism. *Photosynth Res* **109**:47-57.
2. **Whitehead L, Long BM, Price GD, Badger MR.** 2014. Comparing the in vivo function of alpha-carboxysomes and beta-carboxysomes in two model cyanobacteria. *Plant Physiol* **165**:398-411.
3. **Kerfeld CA, Melnicki MR.** 2016. Assembly, function and evolution of cyanobacterial carboxysomes. *Curr Opin Plant Biol* **31**:66-75.
4. **Omata T, Takahashi Y, Yamaguchi O, Nishimura T.** 2002. Structure, function, and regulation of the cyanobacterial high-affinity bicarbonate transporter, BCT1. *Funct Plant Biol* **29**:151-159.
5. **Price G, Woodger F, Badger M, Howitt S, Tucker L.** 2004. Identification of a SulP-type bicarbonate transporter in marine cyanobacteria. *Proc Natl Acad Sci USA* **101**:18228-18233.
6. **Shibata M, Katoh H, Sonoda M, Ohkawa H, Shimoyama M, Fukuzawa H, Kaplan A, Ogawa T.** 2002. Genes essential to sodium-dependent bicarbonate transport in cyanobacteria. *J Biol Chem* **277**:18658-18664.
7. **Shibata M, Ohkawa H, Kaneko T, Fukuzawa H, tabata S, Kaplan A, Ogawa T.** 2001. Distinct constitutive and low-CO<sub>2</sub>-induced CO<sub>2</sub> uptake systems in cyanobacteria: Genes involved and their phylogenetic relationship with homologous genes in other organisms. *Proc Natl Acad Sci* **98**:11789-11794.
8. **Han X, Sun N, Xu M, Mi H.** 2017. Co-ordination of NDH and Cup proteins in CO<sub>2</sub> uptake in cyanobacterium *Synechocystis* sp. PCC 6803. *J Exp Bot* **68**:3869-3877.
9. **Badger MR, Price GD, Long BM, Woodger FJ.** 2006. The environmental plasticity and ecological genomics of the cyanobacterial CO<sub>2</sub> concentrating mechanism. *J Exp Bot* **57**:249-265.
10. **Heinhorst S, Williams E, Cai F, Murin D, Shively J, Cannon G.** 2006. Characterization of the carboxysomal carbonic anhydrase CsoCSA from *Halothiobacillus neapolitanus*. *J Bacteriol* **188**:8087-8094.
11. **Dou Z, Heinhorst S, Williams E, Murin E, Shively J, Cannon G.** 2008. CO<sub>2</sub> fixation kinetics of *Halothiobacillus neapolitanus* mutant carboxysomes lacking carbonic anhydrase suggest the shell acts as a diffusional barrier for CO<sub>2</sub>. *J Biol Chem* **283**:10377-10384.
12. **Sutter M, Roberts EW, Gonzalez RC, Bates C, Dawoud S, Landry K, Cannon GC, Heinhorst S, Kerfeld CA.** 2015. Structural characterization of a newly identified component of alpha-carboxysomes: The AAA plus domain protein CsoCbbQ. *Sci Rep* **5**:16243.
13. **Jannasch H, Wirsén C, Nelson D, Robertson L.** 1985. *Thiomicrospira crunogena* sp. nov., a colorless, sulfur-oxidizing bacterium from a deep-sea hydrothermal vent. *Int J Syst Bacteriol* **35**:422-424.
14. **Dobranski KP, Longo DL, Scott KM.** 2005. A hydrothermal vent chemolithoautotroph with a carbon concentrating mechanism. *J Bacteriol* **187**:5761-5766.
15. **Menning KJ, Menon BB, Fox G, Scott UMLKM.** 2016. Dissolved inorganic carbon uptake in *Thiomicrospira crunogena* XCL-2 is Δp- and ATP-sensitive and enhances RubisCO-mediated carbon fixation. *Arch Microbiol* **198**:149-159.
16. **Dobranski KP, Enkemann SA, Yoder SJ, Haller E, Scott KM.** 2012. Transcription response of the sulfur chemolithoautotroph *Thiomicrospira crunogena* to dissolved inorganic carbon limitation. *J Bacteriol* **194**:2074-2081.
17. **Mangiapi M, MCBL U, Brown T-RW, Chaput D, Haller E, Harmer TL, Hashemy Z, Keeley R, Leonard J, Mancera P, Nicholson D, Stevens S, Wanjugi P, Zabinski T, Pan C, Scott KM.** 2017. Proteomic and mutant analysis of the CO<sub>2</sub> concentrating mechanism of hydrothermal vent chemolithoautotroph *Thiomicrospira crunogena*. *J Bacteriol* **199**:e00871-00816.

18. **Boden R, Scott KM, Williams J, Russel S, Antonen K, Rae AW, Hutt LP.** 2017. An evaluation of *Thiomicrospira*, *Hydrogenovibrio* and *Thioalkalimicrobium*: Reclassification of four species of *Thiomicrospira* to each *Thiomicrothabodus* gen. nov. and *Hydrogenovibrio*, and reclassification of all four species of *Thioalkalimicrobium* to *Thiomicrospira*. *Int J Syst Evol Micro* **67**:1140-1151.
19. **Scott KM, Williams J, Porter CMB, Russel S, Harmer TL, Paul JH, Antonen KM, Bridges MK, Camper GJ, Campa CK, Casella LG, Chase E, Conrad JW, Cruz MC, Dunlap DS, Duran L, Fahsbender EM, Goldsmith DB, Keeley RF, Kondoff MR, Kussy BI, Lane MK, Lawler S, Leigh BA, Lewis C, Lostal LM, Marking D, Mancera PA, McClenthan EC, McIntyre EA, Mine JA, Modi S, Moore BD, Morgan WA, Nelson KM, Nguyen KN, Ogburn N, Parrino DG, Pedapudi AD, Pelham RP, Preece AM, Rampersad EA, Richardson JC, Rodgers CM, Schaffer BL, Sheridan NE, Solone MR, Staley ZR, Tabuchi M, Waide RJ, Wanjugi PW, Young S, Clum A, Daum C, Huntemann M, Ivanova N, Kyrpides N, Mikhailova N, Palaniappan K, Pillay M, Reddy TBK, Shapiro N, Stamatis D, Varghese N, Woyke T, Boden R, Freyermuth SK, Kerfeld CA.** 2018. Genomes of ubiquitous marine and hypersaline *Hydrogenovibrio*, *Thiomicrothabodus*, and *Thiomicrospira* spp. encode a diversity of mechanisms to sustain chemolithoautotrophy in heterogeneous environments. *Environ Microbiol* **20**:2686 – 2708
20. **Nies DH, Koch S, Wachi S, Peitzsch N, Saier MH, Jr.** 1998. CHR, a novel family of prokaryotic proton motive force-driven transporters probably containing chromate/sulfate antiporters. *J Bacteriol* **180**:5799-5802.
21. **Kerfeld CA, Heinhorst S, Cannon GC.** 2010. Bacterial microcompartments. *Ann Rev Microbiol* **64**:391-408.
22. **Merlin C, Masters M, McAteer S, Coulson A.** 2003. Why Is Carbonic Anhydrase Essential to *Escherichia coli*? *J Bacteriol* **185**:6415-6424.
23. **Rosano GL, Ceccarelli EA.** 2014. Recombinant protein expression in *Escherichia coli*: advances and challenges. *Front Microbiol* **5**:172.
24. **Zeebe RE, Wolf-Gladrow D.** 2003. CO<sub>2</sub> in seawater: Equilibrium, kinetics, isotopes. Elsevier, New York.
25. **Knittel K, Kuever J, Meyerdierks A, Meinke R, Amann R, Brinkhoff T.** 2005. *Thiomicrospira arctica* sp. nov. and *Thiomicrospira psychrophila* sp. nov., psychrophilic, obligately chemolithoautotrophic, sulfur-oxidizing bacteria isolated from marine Arctic sediments. *Int J Syst Evol Microbiol* **55**:781-786.
26. **Brinkhoff T, Sievert SM, Kuever J, Muyzer G.** 1999. Distribution and diversity of sulfur-oxidizing *Thiomicrospira* spp. at a shallow-water hydrothermal vent in the Aegean Sea (Milos, Greece). *Appl Environ Microb* **65**:3843-3849.
27. **Axen SD, Erbilgin O, Kerfeld CA.** 2014. A taxonomy of bacterial microcompartment loci constructed by a novel scoring method. *PLoS Comput Biol* **10**: e1003898.
28. **Du J, Förster B, Rourke L, Howitt SM, Price GD.** 2014. Characterisation of cyanobacterial bicarbonate transporters in *E. coli* shows that SbtA homologs are functional in this heterologous expression system. *PLoS ONE* **9**:e115905.
29. **Babu M, Greenblatt JF, Emili A, Strynadka NCJ, Reithmeier RAF, Moraes TF.** 2010. Structure of a SLC26 anion transporter STAS domain in complex with acyl carrier protein: Implications for *E. coli* YchM in fatty acid metabolism. *Structure* **18**:1450-1462.
30. **Price GD, Howitt SM.** 2011. The cyanobacterial bicarbonate transporter BicA: its physiological role and the implications of structural similarities with human SLC26 transporters. *Biochemistry and cell biology = Biochimie et biologie cellulaire* **89**:178-188.
31. **Aravind L, Koonin EV.** 2000. The STAS domain - a link between anion transporters and antisigma-factor antagonists. *Current biology : CB* **10**:R53-55.

- 652 32. **Shelden MC, Howitt SM, Price GD.** 2010. Membrane topology of the cyanobacterial bicarbonate  
653 transporter, BicA, a member of the SulP (SLC26A) family. *Mol Membr Biol* **27**:12-22.
- 654 33. **Price GD, Badger MR, Woodger FJ, Long BM.** 2009. Advances in understanding the  
655 cyanobacterial CO<sub>2</sub>-concentrating-mechanism (CCM): functional components, Ci transporters,  
656 diversity, genetic regulation and prospects for engineering into plants. *J Exp Bot* **59**:1441-1461.
- 657 34. **Le Bris N, Govenar B, Le Gall C, Fisher CR.** 2006. Variability of physico-chemical conditions in 9  
658 degrees 50 ' N EPR diffuse flow vent habitats. *Mar. Chem.* **98**:167-182.
- 659 35. **Markowitz VM, Chen IA, Palaniappan K, Chu K, Szeto E, Pillay M, Ratner A, Huang J, Woyke T,**  
660 **Huntemann M, Anderson I, Billis K, Varghese N, Mavromatis K, Pati A, Ivanova NN, Kyrpides**  
661 **NC.** 2014. IMG 4 version of the integrated microbial genomes comparative analysis system. *Nucl*  
662 *Acids Res* **42**:D560-D567.
- 663 36. **Edgar RC.** 2004. MUSCLE: Multiple sequence alignment with high accuracy and high  
664 throughput. *Nucl Acids Res* **32**:1792-1797.
- 665 37. **Crooks GE, Hon G, Chandonia JM, Brenner SE.** 2004. WebLogo: A sequence logo generator.  
666 *Genome Res* **14**:1188-1190.
- 667 38. **Talavera G, Castresana J.** 2007. Improvement of phylogenies after removing divergent and  
668 ambiguously aligned blocks from protein sequence alignments. *Systematic biology* **56**:564-577.
- 669 39. **Guindon S, Dufayard JF, Lefort V, Anisimova M, Hordijk W, Gascuel O.** 2010. New algorithms  
670 and methods to estimate maximum-likelihood phylogenies: assessing the performance of  
671 PhyML 3.0. *Systematic biology* **59**:307-321.
- 672 40. **Lefort V, Longueville JE, Gascuel O.** 2017. SMS: Smart model selection in PhyML. *Mol Bio Evol*  
673 **34**:2422-2424.
- 674 41. **Le SQ, Gascuel O.** 2008. An improved general amino acid replacement matrix. *Mol Biol Evol*  
675 **25**:1307-1320.
- 676 42. **Rambaut A.** 2016. FigTree: Tree Figure Drawing Tool Version 1.4.3, CoInstitute of Evolutionary  
677 Biology, University of Edinburgh.
- 678 43. **Sorokin DY, Tourova TP, Kolganova TV, Spiridonova EM, Berg IA, Muyzer G.** 2006.  
679 *Thiomicrospira halphila* sp. nov., a moderately halophilic, obligately chemolithoautotrophic,  
680 sulfur-oxidizing bacterium from hypersaline lakes. *Int J Syst Evol Microbiol* **56**:2375-2380.
- 681 44. **Parkhurst DL, Appelo CAJ.** 1999. User's guide to PHREEQC (Version 2) : A computer program for  
682 speciation, batch-reaction, one-dimensional transport, and inverse geochemical calculations.  
683 Report 99-4259.
- 684 45. **Wolery T.** 1979. Calculation of chemical equilibrium between aqueous solution and minerals:  
685 the EQ3/6 software package. [In FORTRAN extended 4. 6 for CDC6600 and 7600].
- 686 46. **Nordstrom DK, Plummer LN, Wigley TML, Wolery TJ, Ball JW, Jenne EA, Bassett RL, Crerar DA,**  
687 **Florence TM, Fritz B, Hoffman M, Holdren GR, Lafon GM, Mattigod SV, McDuff RE, Morel F,**  
688 **Reddy MM, Sposito G, Thraillkill J.** 1979. A comparison of computerized chemical models for  
689 equilibrium calculations in aqueous systems, p. 857-892, *Chemical Modeling in Aqueous*  
690 *Systems*, vol. 93. American Chemical Society.
- 691 47. **Livak KJ, Schmittgen TD.** 2001. Analysis of relative gene expression data using real-time  
692 quantitative PCR and the 2<sup>-ΔΔC<sub>T</sub></sup> method. *Methods* **25**:402-408.
- 693 48. **Wagner S, Klepsch MM, Schlegel S, Appel A, Draheim R, Tarry M, Högbom M, van Wijk KJ,**  
694 **Slotboom DJ, Persson JO, de Gier J-W.** 2008. Tuning *Escherichia coli* for membrane protein  
695 overexpression. *Proc Nat Acad Sci USA* **105**:14371-14376.
- 696 49. **Schlegel S, Löfblom J, Lee C, Hjelm A, Klepsch M, Strous M, Drew D, Slotboom DJ, de Gier J-W.**  
697 2012. Optimizing membrane protein overexpression in the *Escherichia coli* strain Lemo21(DE3). *J*  
698 *Mol Biol* **423**:648-659.

50. **Sagné C, Isambert MF, Henry JP, Gasnier B.** 1996. SDS-resistant aggregation of membrane proteins: application to the purification of the vesicular monoamine transporter. *Biochem J* **316**:825-831.
51. **Sambrook J, Russell DW.** 2001. *Molecular Cloning: A Laboratory Manual*. Cold Spring Harbor Laboratory Press, Cold Spring Harbor.
52. **Oliver DB.** 1996. Periplasm. In Neidhardt FC (ed.), *Escherichia coli* and *Salmonella*: Cellular and Molecular Biology, vol. 1. ASM Press, Washington, DC.
53. **Davanloo P, Rosenberg AH, Dunn JJ, Studier FW.** 1984. Cloning and expression of the gene for bacteriophage T7 RNA polymerase. *Proc Natl Acad Sci U S A* **81**:2035-2039.
54. **Cervantes C, Ohtake H, Chu L, Misra TK, Silver S.** 1990. Cloning, nucleotide sequence, and expression of the chromate resistance determinant of *Pseudomonas aeruginosa* plasmid pUM505. *J Bacteriol* **172**:287-291.
55. **Zolotarev AS, Unnikrishnan M, Shmukler BE, Clark JS, Vondorpe DH, Grigorieff N, Rubin EJ, Alper SL.** 2008. Increased sulfate uptake by *E. coli* overexpressing the SLC26-related SulP protein Rv1739c from *Mycobacterium tuberculosis*. *Comparative biochemistry and physiology. Part A, Molecular & integrative physiology* **149**:255-266.
56. **Weissgerber TL, Milic NM, Winham SJ, Garovic VD.** 2015. Beyond bar and line graphs: time for a new data presentation paradigm. *PLoS Biol* **13**:e1002128.
57. **Goffredi SK, Childress JJ, Desaulniers NT, Lee RW, Lallier FH, Hammond D.** 1997. Inorganic carbon acquisition by the hydrothermal vent tubeworm *Riftia pachyptila* depends upon high external P-CO<sub>2</sub> and upon proton-equivalent ion transport by the worm. *J Exp Biol* **200**:883-896.
58. **Ahmad A, Barry JP, Nelson DC.** 1999. Phylogenetic affinity of a wide, vacuolate, nitrate-accumulating *Beggiatoa* sp. from Monterey Canyon, California, with *Thioploca* spp. *Appl Environ Microbiol* **65**:270-277.

## FIGURE LEGENDS

**FIG 1** Carboxysome-associated locus and genome context among members of genus *Thiomicrospira*. Homologous genes are consistently colored among genomes. Black genes are unique to the genome within the region depicted. For *Tmr. chilensis*, dots indicate a region of the scaffold that has not been sequenced. Locus tags depicted are A379DRAFT\_1550 – 1580 (*Tmr. frisia* KP2), BS34DRAFT\_2186 – 2175 (*Thiomicrospira* sp. Milos-T2), F612DRAFT\_1864 – 1855 (*Tmr. arctica*), and B076DRAFT\_0150 – 0174 (*Tmr. chilensis*). The phylogenetic tree on the left is a portion of a larger phylogenetic analysis in (19).

734

735 **FIG 2** Maximum likelihood analysis of homologs of Tcr\_0853 and 0854 (A), and  
 736 members of the Chr (B) transporter family. Borders highlight members of  
 737 *Thiomicrospira*, *Hydrogenovibrio*, and *Thiomicrothrix*; 'Q+' and 'Q-' indicate genes  
 738 whose transcripts were assayed via qRT-PCR and found to be upregulated, or not,  
 739 respectively, under low-DIC conditions (Table 2). 'E' indicates genes heterologously  
 740 expressed in *E. coli*. Taxon names are preceded by Integrated Microbial Genomes  
 741 gene object id numbers or GenBank accession numbers, and are also preceded by 'BC'  
 742 when the gene products have been characterized biochemically (54). When transporter  
 743 family genes were collocated with genes encoding enzymes that consume or produce  
 744 DIC, taxon names are preceded by the following abbreviations: CA – carbonic  
 745 anhydrase; cbbM – form II RubisCO; CS – carboxysome; FDH – formate  
 746 dehydrogenase; OAOR – oxoacid: acceptor oxidoreductase. In (A), '3sub' indicates that  
 747 a gene encoding a potential third subunit is present between genes encoding homologs  
 748 of Tcr\_0853 and 0854. Alignments had 420 (A) and 138 (B) positions. Bootstrap  
 749 values >65% from 1000 resamplings of the alignment are shown, and the trees are  
 750 unrooted. The scale bar represents the number of substitutions per site.

751

752 **FIG 3** Maximum likelihood analysis of homologs of SbtA (A) and SulP (B) transporter  
 753 families. Borders highlight members of *Thiomicrospira*, *Hydrogenovibrio*, and  
 754 *Thiomicrothrix*; 'Q+' and 'Q-' indicate genes whose transcripts were assayed via  
 755 qRT-PCR and found to be upregulated, or not, respectively, under low-DIC conditions  
 756 (Table 2). 'E' indicates genes heterologously expressed in *E. coli*. Taxon names are

preceded by Integrated Microbial Genomes gene object id numbers or GenBank accession numbers, and are also preceded by 'BC' when the gene products have been characterized biochemically (28, 29, 55). When transporter family genes were collocated with genes encoding enzymes that consume or produce DIC, taxon names are preceded by the following abbreviations: CA – carbonic anhydrase; cbbL – form I RubisCO; cbbM – form II RubisCO; CS – carboxysome; FHL – formate hydrogen lyase; OAOR – oxoacid: acceptor oxidoreductase; PUR – purine biosynthesis; PyrC – pyruvate carboxylase. ). Alignments had 148 (A), and 160 (B) positions. Bootstrap values >65% from 1000 resamplings of the alignment are shown, and the trees are unrooted. The scale bar represents the number of substitutions per site.

**FIG 4** Growth of *Hydrogenovibrio* (A), *Thiomicrothrix*, and *Thiomicrospira* (B) species under low DIC conditions. Single cultures from each species were cultivated under an ambient headspace with 2 mM DIC. *Tmr. arctica* was cultivated at 10°C; the rest were grown at 20°C.

**FIG 5** Transmission electron micrographs of cells exposed to low-DIC conditions to induce carboxysome synthesis. Carboxysomes are visible as 0.1 µm electron-dark inclusions; when present in the cells, two are indicated per cell with arrows.

**FIG 6** Intracellular DIC accumulation by *E. coli* expressing potential DIC transporter genes A) Tcr\_0853, Tcr\_0854, or *chr*, and B) *sbtA* or *sulP*. (F) or (R) following gene



names indicates the orientation of the gene (forward or reverse) with respect to the T7 promoter. '8534' is a construct carrying both Tcr\_0853 and Tcr\_0854, while '0853' and '0854' each carry Tcr\_0853 or Tcr\_0854 respectively. DIC concentrations were measured 8 times for cells from a single culture of each construct, and the median value for each construct is indicated with a short horizontal bar. The concentration of extracellular DIC was 0.25 mM, and the incubation time was 90 sec. Asterisks indicate constructs in which genes in forward orientation accumulated DIC to a significantly higher concentration than when in reverse orientation ( $\alpha < 0.05$ ). Scatterplots of intracellular DIC pools were generated using the template provided in (56).

**FIG 7** Growth of carbonic anhydrase-deficient *E. coli* EDCM636 under ~400 ppm CO<sub>2</sub> when expressing candidate DIC transporters. Cells were cultivated in the presence of 0.4 mM IPTG, unless indicated otherwise ('- IPTG'). Genes encoding potential DIC transporters were oriented in forward (F) or reverse (R) orientation relative to the T7 promoter driving expression. A. Cells carrying Tcr\_0853 (853), Tcr\_0854 (854), or both (8534). B and C. Replicate experiments for cells expressing *chr* genes. D and E. Cells expressing *sbt* or *sulP* genes, respectively.

**FIG 8** Model of DIC transporter gene acquisition, loss, and changes in genome location. The sequence of events with the least number of gene gains, losses, and movements within the chromosome is presented, overlaying a ribosome-protein based supertree (19) of the organisms. Asterisks mark clades with 98 – 100 % bootstrap

801 support. On the left is a possible ancestral carboxysome locus. On the right are the  
802 carboxysome loci in these organisms. Numbers in parentheses indicate the number of  
803 scaffolds of the draft genome sequence; (C) indicates that the genome sequence is  
804 complete. + *gene* = phylogenetic analysis and gene taxonomic distribution suggest  
805 acquisition via horizontal gene transfer; - *gene* = gene is absent from sequenced  
806 genome; CS = gene is collocated with carboxysome locus; to CS = gene moved from  
807 elsewhere in the chromosome, to collocation with carboxysome locus; CCM = CO<sub>2</sub>  
808 concentrating mechanism.

809

810

811

812 **TABLE 1** Dissolved inorganic carbon speciation in *Tmr. arctica* and *H. crunogenus*  
813 habitats

	Arctic marine sediments <sup>a</sup> ( <i>Tmr. arctica</i> )	Hydrothermal vents <sup>a</sup> ( <i>H. crunogenus</i> )
Temperature	0.01 – 6.00 °C	2.00 – 20.00 °C
pH	8.22	7.20 - 5.60
Sulfide <sup>b</sup>	0 – 0.3	0 – 0.3
DIC	2.32	2.7 – 7.1
CO <sub>2</sub>	0.017 – 0.015	0.194 – 5.157
HCO <sub>3</sub> <sup>-</sup>	1.062 – 1.344	1.483 – 1.029
NaHCO <sub>3</sub>	0.464 – 0.627	0.682 – 0.326
MgHCO <sub>3</sub> <sup>+</sup>	0.167 – 0.206	0.232 – 0.153
CaHCO <sub>3</sub> <sup>+</sup>	0.030 – 0.037	0.041 – 0.028
CO <sub>3</sub> <sup>2-</sup>	0.012 – 0.022	0.002 – 0.000
NaCO <sub>3</sub> <sup>-</sup>	0.007 – 0.011	0.001 – 0.000
MgCO <sub>3</sub>	0.023 – 0.047	0.004 – 0.001
CaCO <sub>3</sub>	0.007 – 0.015	0.001 – 0.000

814  
815 <sup>a</sup>Temperatures, pH, sulfide, and DIC from Arctic marine sediments and hydrothermal  
816 vents are based on those present at the locations from which these organisms were  
817 isolated (25, 34, 57, 58).

818 <sup>b</sup>Compounds are presented in mM

**TABLE 2** Transcript abundances of genes encoding carboxysome components and potential DIC transporters in members of the genera *Hydrogenovibrio*, *Thiomicrobacter*, and *Thiomicrospira*

Taxon	Genes <sup>a</sup>	$\alpha$ ( $-\Delta\Delta C_t = 0$ ) <sup>b</sup>	$-\Delta\Delta C_t \pm SD^c$	$\alpha$ ( $-\Delta\Delta C_t > 1$ ) <sup>d</sup>	Fold increase (low DIC/high DIC)
<i>Hydrogenovibrio</i> <i>crunogenus</i> XCL-2	<i>csoS3</i>		$9.7 \pm 1.9^e$		823
	853-I (CS)		$8.0 \pm 1.8^e$		263
	854-I (CS)		$8.4 \pm 1.6^e$		340
	<i>chr-I</i>	- <sup>f</sup>	$0.4 \pm 0.7$		1.3
	<i>sulP-II</i>	<0.05	$0.8 \pm 0.2$	N/A <sup>g</sup>	1.8
<i>Hydrogenovibrio</i> <i>thermophilus</i> JR2	<i>csoS3</i>	<0.005	$11.0 \pm 0.2$	<0.001	1984
	<i>chr-I</i> (CS)	<0.005	$6.8 \pm 0.2$	<0.001	114
	853-I	<0.005	$10.2 \pm 0.3$	<0.001	1181
	854-I	<0.005	$8.7 \pm 0.1$	<0.001	413
	<i>sulP-I</i>	<0.005	$6.9 \pm 0.1$	<0.001	123
	<i>sulP-II</i>	<0.01	$-1.1 \pm 0.1$	N/A	0.5
<i>Hydrogenovibrio</i> <i>thermophilus</i> MA2-6	<i>csoS3</i>	<0.005	$12.5 \pm 0.4$	<0.001	5746
	<i>chr-I</i> (CS)	<0.005	$6.2 \pm 0.4$	<0.005	73
	853-I	<0.005	$6.4 \pm 0.4$	<0.001	85
	854-I	<0.005	$8.2 \pm 0.4$	<0.001	289
	<i>sulP-II</i>	-	$-0.1 \pm 0.5$	N/A	0.9
<i>Hydrogenovibrio</i> <i>halophilus</i>	<i>csoS3</i>	<0.005	$11.3 \pm 0.3$	<0.001	2517
	<i>sbtA-I</i> (CS)	<0.005	$9.4 \pm 0.2$	<0.001	680
	<i>chr-I</i>	<0.05	$-0.5 \pm 0.2$	N/A	0.7
	<i>sulP-III</i>	<0.05	$-0.8 \pm 0.2$	N/A	0.6

<i>Hydrogenovibrio marinus</i>					
	<i>csoS3</i>	<0.005	8.4 ± 0.4	<0.001	340
	853-I (CS)	<0.005	5.9 ± 0.4	<0.001	61
	854-I (CS)	<0.01	4.1 ± 0.3	<0.005	18
	<i>chr-II</i>	-	-0.9 ± 0.5	N/A	0.5
<i>Hydrogenovibrio</i> sp. Milos-T1					
	<i>csoS3</i>	<0.005	4.8 ± 0.2	<0.001	28
	853-I (CS)	<0.005	3.5 ± 0.2	<0.001	11
	854-I (CS)	<0.01	5.1 ± 0.4	<0.005	33
	853-II	<0.01	2.7 ± 0.2	<0.005	6
	<i>hyp</i> (853)	<0.005	4.1 ± 0.2	<0.005	17
	854-II	<0.005	4.1 ± 0.3	<0.005	17
	<i>chr-II</i>	-	-0.3 ± 0.2	N/A	0.8
<i>Thiomicrothrix frisia</i> Kp2					
	<i>csoS3</i>	<0.005	12.4 ± 0.3	<0.001	5327
	<i>sbtA-I</i> (CS)	<0.05	9.2 ± 0.6	<0.025	597
	<i>sulP-II</i>	<0.05	1.4 ± 0.4	-	2.7
<i>Thiomicrospira pelophila</i>					
	<i>csoS2</i>	<0.025	1.8 ± 0.3	<0.05	3
	<i>hyp</i> ( <i>csoS2</i> )	N/A	ND <sup>h</sup>	N/A	
	<i>sulP-I</i> (CS)	<0.025	1.6 ± 0.4	-	3
	<i>sbtA-I</i> (CS)	<0.01	2.2 ± 0.3	<0.01	5
	853-I	<0.005	6.4 ± 0.4	<0.001	99
	854-I	<0.005	6.2 ± 0.4	<0.001	73
	<i>chr-I</i>	-	-0.2 ± 0.3	N/A	1
	<i>sbtA-II</i>	<0.05	10.4 ± 2.7	<0.025	1391
	<i>sulP-III</i>	-	-0.1 ± 0.5	N/A	0.9

822

823 <sup>a</sup>Gene abbreviations: *chr* = chromate ion transporter family; *sulP* = sulfate transporter family; 853, 854 = homologs to

824 Tcr\_0853, 0854; *hyp*(*x*) = hypothetical protein adjacent to gene *x*; *sbtA* = sodium-dependent bicarbonate transporter

825 family. Roman numerals (I, II, III) are consistent with the clades labeled in Fig. 2 and 3. (CS) indicates that the genes are  
826 adjacent to the carboxysome locus. IMG gene object ID numbers for all genes targeted here are listed in Table 4.

827 <sup>b</sup>For all species, citrate synthase was used as the calibrator gene.

828 <sup>c</sup>two-tailed *t*-test, n=3 for all except *Tmr. frisia* Kp2 *sbtA* (CS), for which n=2

829 <sup>d</sup>one-tailed *t*-test, n=3 for all except *Tmr. frisia* Kp2 *sbtA* (CS), for which n=2

830 <sup>e</sup>(17)

831 <sup>f</sup> -:  $\alpha > 0.05$

832 <sup>g</sup>N/A: Not applicable

833 <sup>h</sup>ND: Not detectable; C<sub>t</sub> values similar to cDNA-free controls (>30). Primers successfully amplified this target when gDNA  
834 was the template.

835

**TABLE 3** Detection of putative DIC transporter proteins when heterologously expressed in *E. coli*

Sample <sup>a</sup>	Strain	Protein	Intensity	Unique Peptides	Sequence Coverage (%)
8534	<i>Hydrogenovibrio crunogenus</i> XCL-2	Tcr_0853	1.37E+09	5	11.4
		Tcr_0854	7.12E+11	57	76.7
853	<i>Hydrogenovibrio crunogenus</i> XCL-2	Tcr_0853	4.30E+07	2	4.4
854	<i>Hydrogenovibrio crunogenus</i> XCL-2	Tcr_0854	2.69E+10	35	60.9
Chr	<i>Hydrogenovibrio thermophilus</i> JR2	Chr	2.56E+09	5	16.9
SbtA	<i>Thiomicrospira</i> Kp2	SbtA	5.49E+09	4	7.5
SulP	<i>Hydrogenovibrio thermophilus</i> JR2	SulP	6.21E+08	2	5.4

<sup>a</sup>Samples consisted of membranes prepared from *E. coli* cells expressing potential DIC transporters. Sample 8534 is from *E. coli* expressing both Tcr\_0853 and Tcr\_0854 (8534), while samples 853 and 854 were from *E. coli* expressing either Tcr\_0853 or Tcr\_0854.

845

846

847

848

849

850

851



852 **TABLE 4** Primers used for qRT-PCR

<b>Taxon</b>	<b>IMG gene object ID<sup>a</sup></b>	<b>Predicted gene product<sup>b</sup></b>	<b>Forward primer</b>	<b>Reverse primer</b>
<i>H. crunogenus</i> XCL-2	637785059	Citrate synthase	CTTTGATGCGGGCTTGTTTAC	CCCCTGTGTAGATTTGAGTCG
	637785561	CsoSCA	CTCCGCTTACCTTATGCCTTAG	AGTAACGTGTTGGTTCATCCG
	637786436	Chr-I	GGTTTCGGCCTGGACTATTT	GCGCTTCATCAAACCAAGAC
	637786269	SulP-II	CGGATTGATTACCGCCATCT	TGCCATGCTCCATCACTAAA
<i>H. thermophilus</i> JR2	2507072380	Citrate synthase	CGAATCCGTGCTCGGTTATT	GAACCGATTTTCATCCAGCATTTTC
	2507073759	CsoSCA	GCGTTCCAGGCTCTAAAGATAG	GGATGCCGACAATTCCTGATA
	2507073746	Chr-I (CS)	GCTGGAGCTTGATCGTGTTA	CCATCTCCGATCGACCAAATAC
	2507074342	853-I	CCTGTTTATGGCCGGTTACA	GTCACCCATTTCGTCCAGATAAA
	2507074343	854-I	GCTTCGCCTCAGTGTCTATATC	GAGTCCCAACGGAAACAGAA
	2507074344	SulP-I	TGTGTGGCTGTGGCTTTAT	TTGGAGTTACAGGGTCGTTTC
	2507073582	SulP-II	ACACCTTGTCGGGCATTAC	GAGGTGATGAAACCGACGATAA
<i>H. thermophilus</i> MA2-6	2572250326	Citrate synthase	CGAATCCGTGCTCGGTTATT	GAACCGATTTTCATCCAGCATTTTC
	2572249265	CsoSCA	GAAATCGGAAGACAGGACAGAG	CCATTTTCATAACGACGCAACAA
	2572249252	Chr-I (CS)	TGGCGCTGAATCTGGTATTG	CGCCACCCAACTCCAATAAA
	2572249866	853-I	CCTACATGGCCGGAATAAG	ATCCAAGCGGTCATCATCAG
	2572249867	854-I	ATGTGCGCTCGGAAATCA	GGGCGGTATTCTATCGGTAATC
	2572249063	SulP-II	ACACCTTGTCGGGCATAAC	GACGATAATCGCGGCATACA
<i>H. halophilus</i>	2518266203	Citrate synthase	CCAGACGGGTCAAATACAATCT	ATGTATTCCGGTGCTGGGATAAA
	2518265324	CsoSCA	AGGGTCTGTACCCGGATATT	CGTGTCCAGAAACCCGTAAT
	2518265315	SbtA-I (CS)	ATTGGCCACGTCGGATTT	GAATCGCAACAGCGCATAAC
	2518266741	Chr-I	CTGGCTGGGACAAACCTATT	CCCAGAGCCGAACCTCATTT
	2518265727	SulP-III	TGGCCGGGTATCTGAATTTG	CGGTAGCTGAGCCATGAATATC
<i>H. marinus</i>	2574157295	Citrate synthase	AGAAGAGTTGGGAGCGTTTG	GGATGTGTTGTTGACGGTAGAT
	2574157483	CsoSCA	CGTTATCAGGAGTTGTCGGTATC	CTGCCAGGTTGGGTAGTTT

	2574157469	853-I (CS)	GCGGCACTGCTATTTGTTTAC	ACTGATCCACAGGTCTCCTATC
	2574157468	854-I (CS)	TTATGACTGGCAGCAGGATAAG	CGACGCGTAGTACTGAAGATTG
	2574158185	Chr-II	TGCTGCTGGTCTGCTATTT	CGGGCTTAATGCCGTAGAA
<i>Hydrogenovibrio</i> sp. Milos-T1	2579718736	Citrate synthase	GACTGGTGAAGAGCCAGATAAG	CCCAGTCACCATAGTGGTAAAG
	2579719002	CsoSCA	GATGTCAGCGAGAGTGTTAGAG	TCTGCTTTTCGAGAAGTGGTAAA
	2579719013	853-I (CS)	GGGATTTGTGGATGGCATTTC	ACACTCTTCTGGTCTTCATCATC
	2579719014	854-I (CS)	GGGATGTATAGCGAGTGGTTAG	GGTATCTGGCAAGCTGAGAA
	2579719194	853-II	GTTTGGCGAGCAGCTTTATG	CCCGTAGCCAGCCAATAATAA
	2579719193	Hyp(853)	TCCTAACTGGGTGATGATTTGG	CATGCAGACGTCGCAATAAAG
	2579719192	854-II	ACTACCAACCCAAGCCTAAAG	GTAGTCTCCCATGCCTTCTAAAT
	2579720167	Chr-II	CATCAGGAGCTGGTGGATAAG	ATATAGGTGGCGAGCTGTTG
<i>Tmr. frisia</i> Kp2	2517375157	Citrate synthase	ACCCTTGTTTCGGTTATCTCTTC	CAGGCGAACCAATCTCATCT
	2517375722	CsoSCA	GCGTACGTAACTGGGTCTTTAT	TTGGTGGTGTGGATCTGATTT
	2517375731	SbtA-I (CS)	GCACACGAAAGCTACCCTATTA	CTGAGAACCATCACCTGAAGTC
	2517376429	SulP-II	ATGACACCCTATCAGGCATTAC	CAGGACGACCACCAATAACA
<i>Tms. pelophila</i>	2568511528	Citrate synthase	GATCCAATTGAACCGCGTAAAG	CATCAAGTAAACGTGCCCAATC
	2568509998	CsoS2	GCTAATGCTTACTCTGCACCTA	CGGCTCCATCTCCTGTTATTC
	2568509999	Hyp(csoS2)	TAGGTTGCGCCAAGCAGTAAG	GCATCAGTCAAGGCATACAAAC
	2568510006	SulP-I (CS)	GAAGCGCCTAAACAAGACAAAG	TAGCCATTGCGGCTGTAATAA
	2568510007	SbtA-I (CS)	GCGGCTAGTGCATCCTATATT	ACGGAAAGGTAACCTCCAAGTG
	2568511025	853-I	CGGGTAATGTTGAGGAAGAGAA	AACCCACGCCAGCATAAA
	2568511024	854-I	GGAGTCCAACCTTAGCCGATTAC	AGCCCGTCTTGCCAATTTA
	2568510063	Chr-I	CGCCGCCTTAATAAATCCAATC	AACAGGTTTCAGACCCAGTAATC
	2568511393	SbtA-II	GCGGCTACCTATGGTTCAATTA	ACCATTGCCACCGTCATATAG
	2568511001	SulP-III	GTCAGGGCGTGGCAAATA	CCTGCCGTAAAGGTGGATAAA

853

854 <sup>a</sup>Gene object identification numbers from the Integrated Microbial Genomes system ([https://img.jgi.doe.gov/cgi-](https://img.jgi.doe.gov/cgi-bin/m/main.cgi)  
855 [bin/m/main.cgi](https://img.jgi.doe.gov/cgi-bin/m/main.cgi))

856 <sup>b</sup>Gene product abbreviations: CsoSCA = carboxysomal carbonic anhydrase; Chr = chromate ion transporter family; SulP  
857 = sulfate permease family; 853, 854 = homologs to proteins encoded by *Tcr\_0853*, *0854*; Hyp(x) = hypothetical protein  
858 adjacent to gene x; SbtA = sodium-dependent bicarbonate transporter family. Roman numerals after predicted gene  
859 product names indicate the clade in which the gene is found (Fig. 2, Fig. 3). Gene product names followed by (CS)  
860 indicate that these genes are adjacent to those encoding the components of carboxysomes.

861

862

863 **TABLE 5** Primers used for heterologous expression of potential DIC transporters

<b>Taxon</b>	<b>IMG gene object ID<sup>a</sup></b>	<b>Predicted gene product<sup>b</sup></b>	<b>Forward primer</b>	<b>Reverse primer</b>
<i>H. crunogenus</i> XCL-2	637785573	853 (CS)	CACCATGAATATGCAATGGGTAGG	TCATTGAAATAACTCCTCTTTAGGAACTT
	637785574	854 (CS) 853 & 854	CACCATGATGTTGCACAACGC CACCATGAATATGCAATGGGTAGG	TCAGGCAGATTCCAACCACT TCAGGCAGATTCCAACCACT
<i>H. thermophilus</i> JR2	2507073746	chr (CS)	CACCATGTCATTGCCTGTCTTTTG	TTAGCCCGAAACAAACGACACC
		chr (reverse)	ATGTCATTGCTTGTCTTTTGGC	CACCTTAGCCCGAAACAAACG
	2507074344	SulP SulP (reverse)	CACCATGACACAGGAAAACATAAAC ATGACACAGGAAAACATAAACACAG	TCAATTTAATTCTTTATCGTCTTCTTTAAATTTTTTG CACCTCAATTTAATTCTTTATCGTCTTCTTTAA
<i>Tmr. frisia</i> Kp2	2517375731	SbtA (CS)	CACCATGTTGGGATTGGATAGC	TTATACCGCTGAATACCACATAGC

864

865 <sup>a</sup>Gene object identification numbers from the Integrated Microbial Genomes system ([https://img.jgi.doe.gov/cgi-](https://img.jgi.doe.gov/cgi-bin/m/main.cgi)  
866 [bin/m/main.cgi](https://img.jgi.doe.gov/cgi-bin/m/main.cgi))

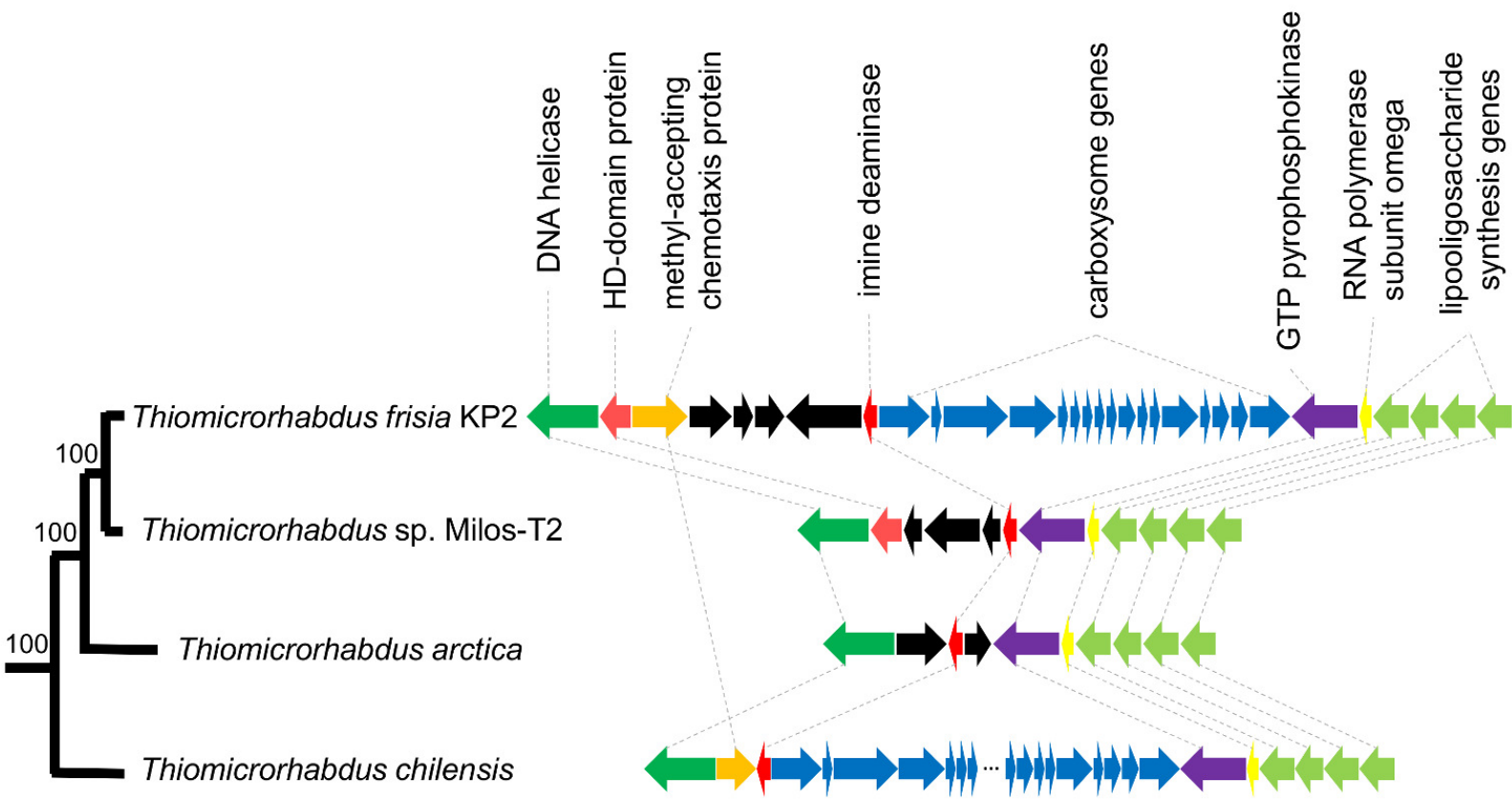
867 <sup>b</sup>Gene product abbreviations: Chr = chromate ion transporter family; SulP = sulfate permease family; 853, 854 = proteins  
868 encoded by Tcr\_0853, 0854; SbtA = sodium-dependent bicarbonate transporter family. Gene product names followed by  
869 (CS) indicate that these genes are adjacent to those encoding the components of carboxysomes.

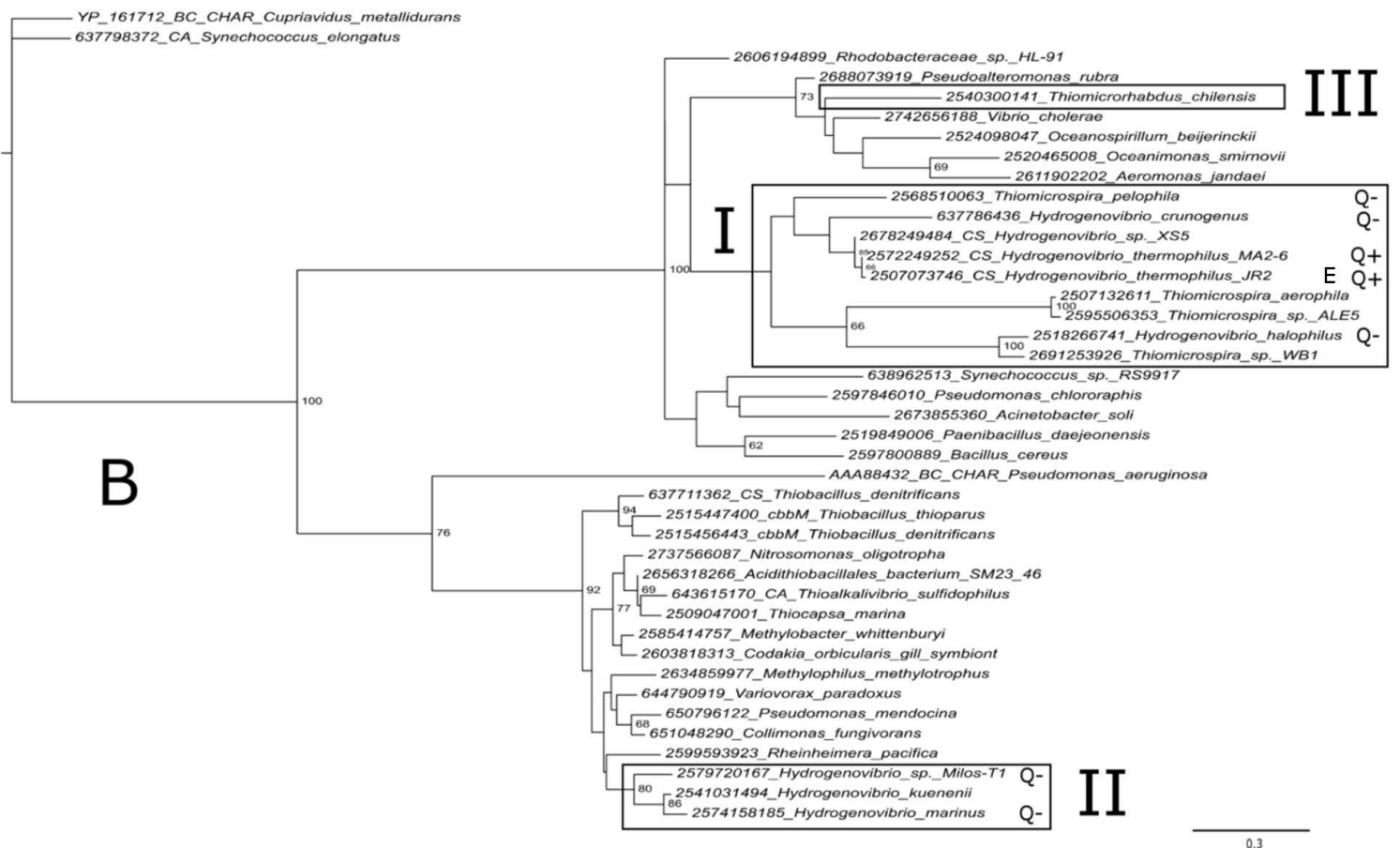
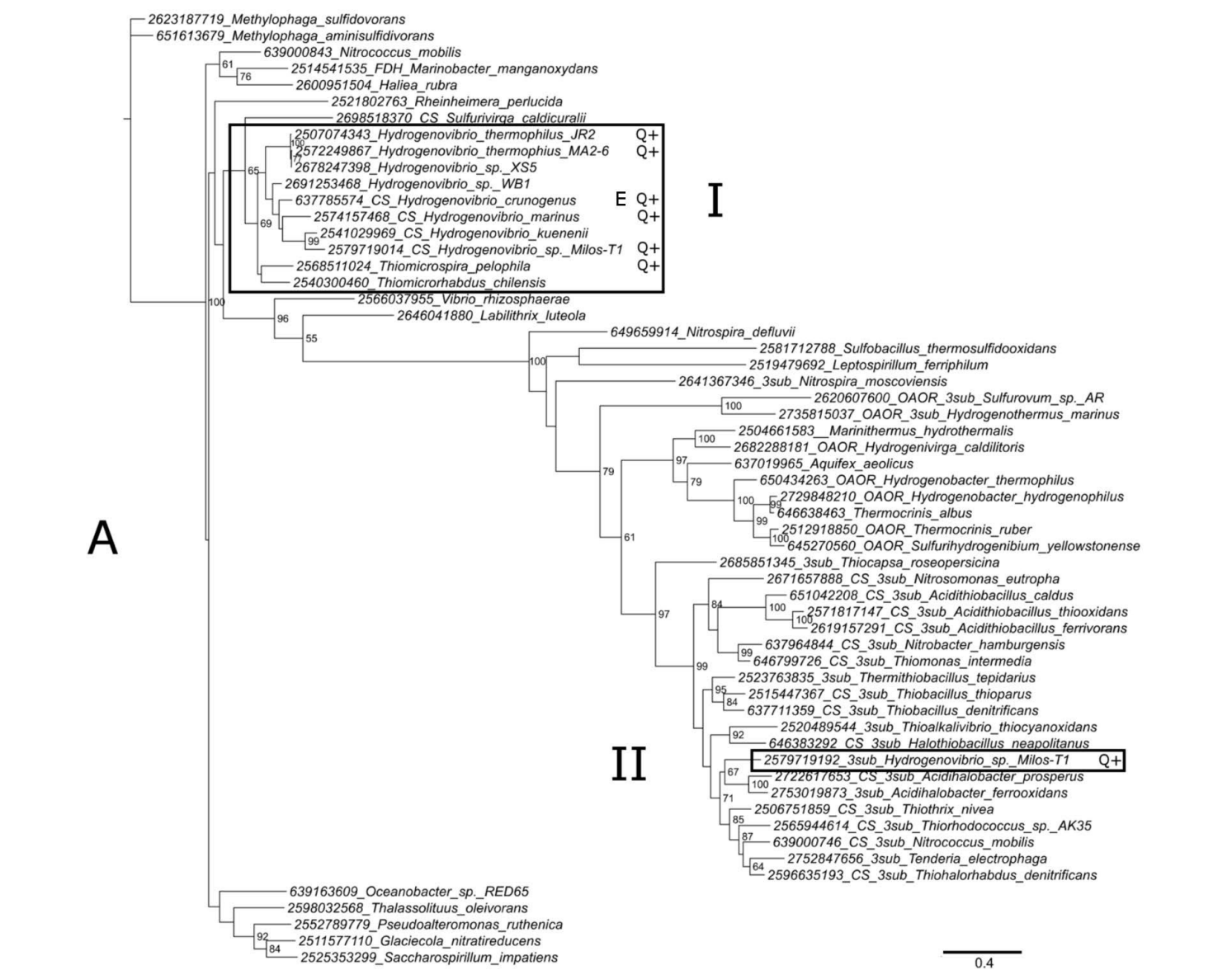
870

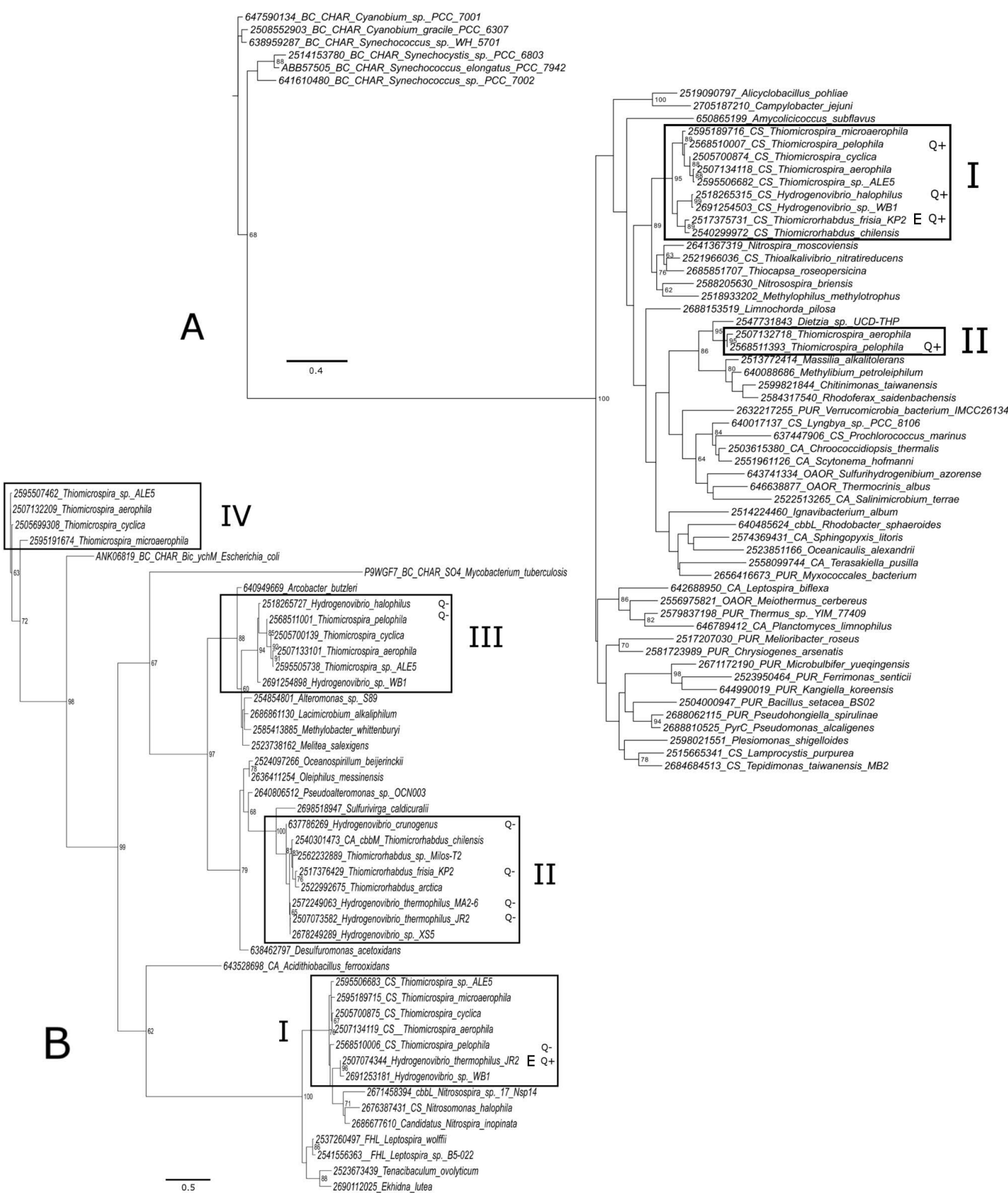
871

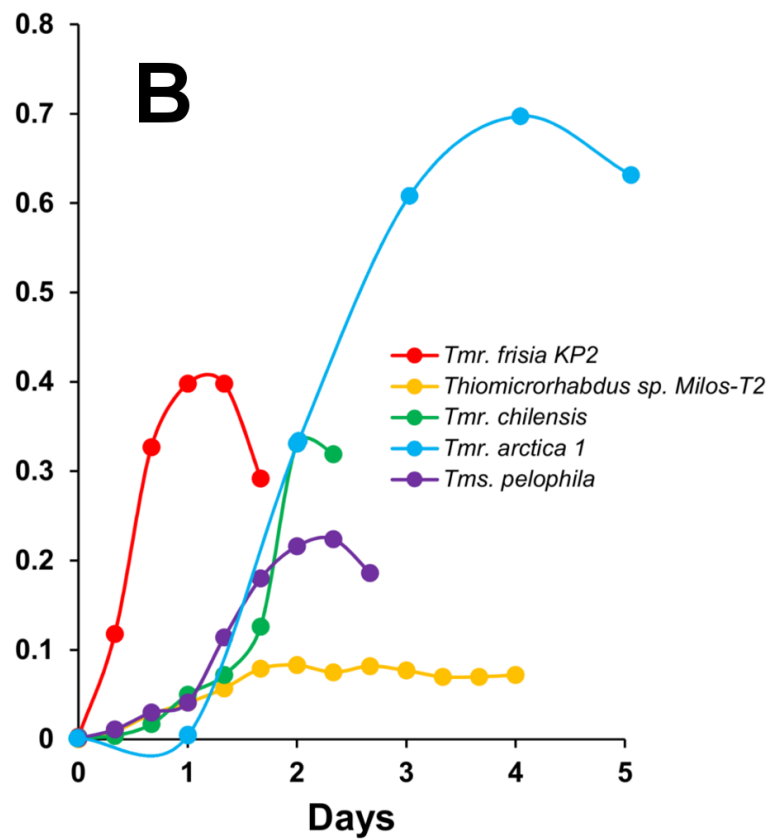
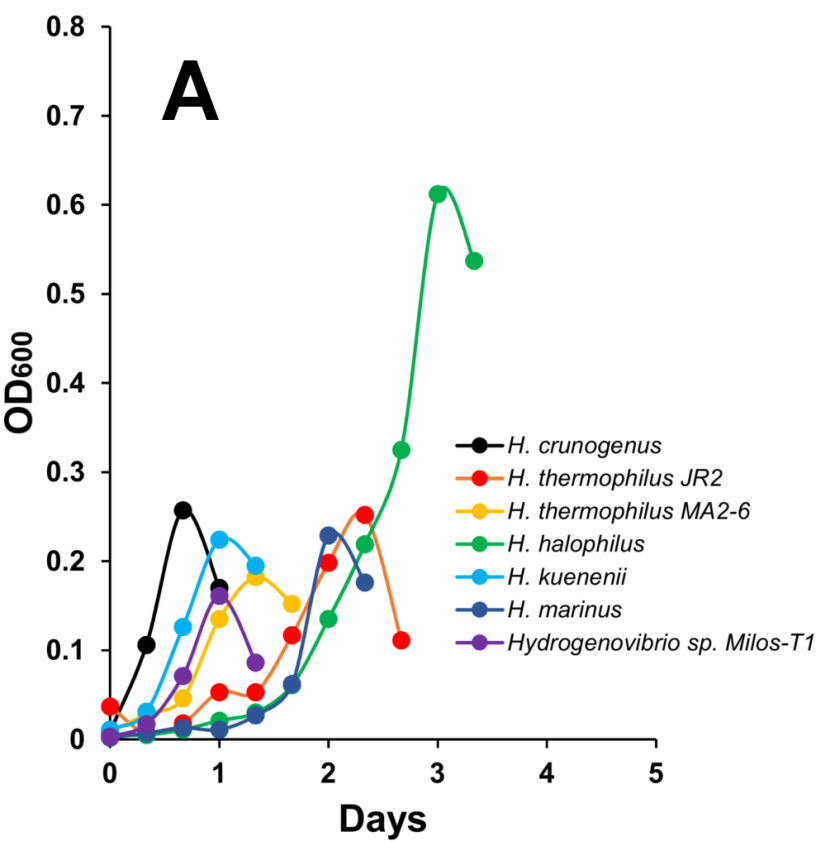
872

873

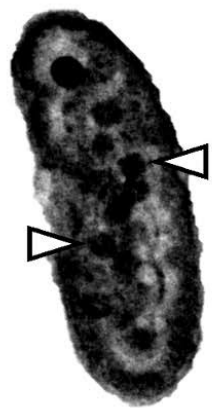








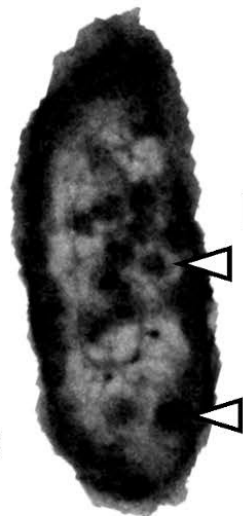




*H. crunogenus*



*H. thermophilus*  
JR2



*H. thermophilus*  
MA2-6



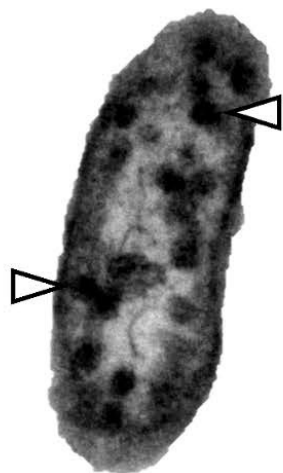
*H. kuenenii*



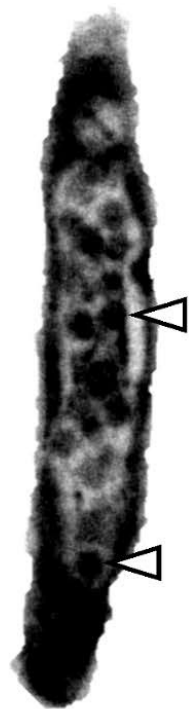
*H. halophilus*



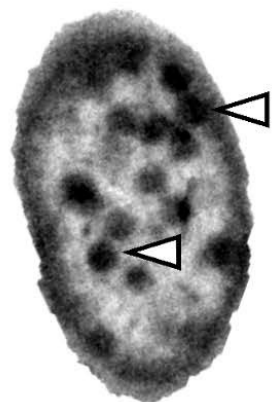
*Thiomicrobacter* sp.  
Milos T2



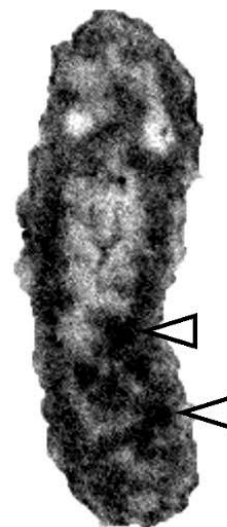
*H. marinus*



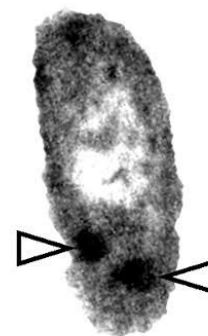
*Hydrogenovibrio* sp.  
Milos T1



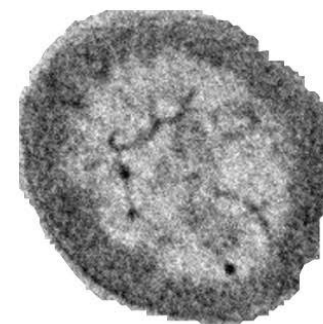
*Tmr. frisia* Kp2



*Tmr. chilensis*



*Tms. pelophila*

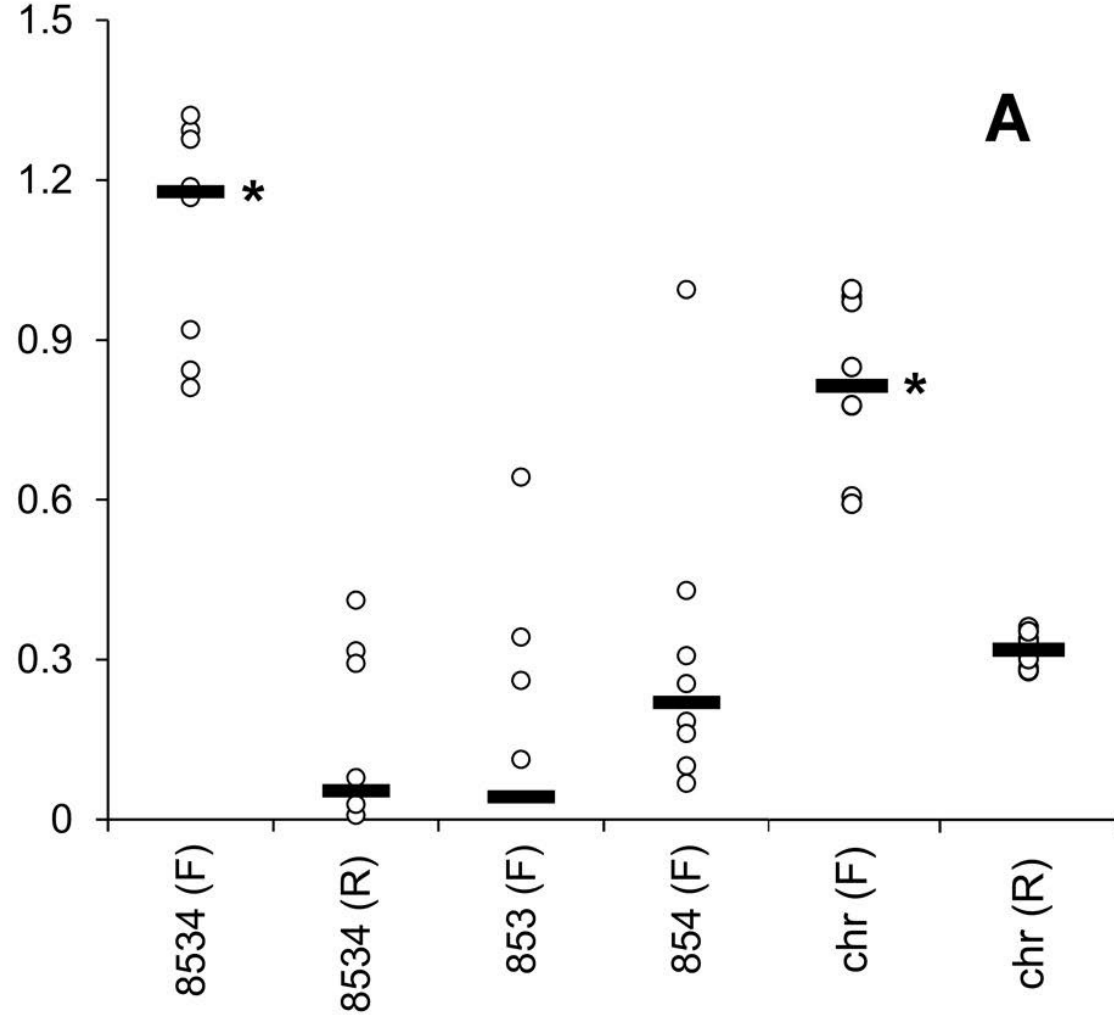


*Tmr. arctica*



2 μm

Intracellular DIC (mM)



Intracellular DIC (mM)

